

VALIDATION OF AN INSTRUMENTATION MODULE
USING RATE GYROS AND LINEAR ACCELEROMETERS
FOR BIOMECHANICAL APPLICATIONS

Anthony S. Hu, Sc.D.

Physical Science Laboratory

New Mexico State University

Las Cruces, New Mexico 88003

Abstract

Three dimensional kinematic measurement in biomechanical experiments has always been a difficult task. This paper presents the validation results and related studies of a six degree-of-freedom instrumentation module using three rate gyros and three linear accelerometers. A technique of coordinate rotation using only rate gyro data is derived. Methods of taking derivatives and their frequency bandwidth relationships are discussed. Finally, the kinematic effect due to module weight (0.75 lbs) using experiment and computer model methods are presented. The results, as compared with the film data, indicated that good kinematic correlations can be obtained. This instrumentation module may be considered as a viable tool in biomechanical research.

INTRODUCTION

In biomechanical experiments, a commonly used instrument for kinematic measurement is the nine-accelerometer instrumentation module [1]. This module

utilizes nine linear accelerometers arranged in an ingenious 3-2-2-2 configuration, thus providing three elegant linear equations which relate the accelerometer measurements to the angular accelerations of the module. However, since this module measures the differences between paired accelerations while the accelerometers undergo impact environment, this requires extremely accurate accelerometer tracking (differential) data. The precision alignment and the complicated calibration procedures also require special attention. The size reduction is restricted because the calculated angular acceleration error is inversely proportional to the size of the module. Furthermore, a set of angular kinematic measurements consists of angular acceleration as well as angular velocity and angular displacement. It is especially important for the angular displacement (which is obtained by double integrating the angular acceleration data) since double integration accumulates errors proportional to time squared.

The purpose of this paper is to present the first-phase test results of a Rate-Gyro-Linear-Accelerometer (RGLA) inertial module which may be considered as an alternative to the nine-accelerometer module. This paper presents the validation results in 2-D and 3-D models. A technique of coordinate rotation using only rate gyro data is derived. Methods of taking derivatives and their frequency bandwidth relationships are also discussed. Finally, the change of kinematic responses due to the additional module weight is presented.

THE RGLA MODULE

The complete six-degree-of-freedom (three rotational and three translational kinematic measurements) Rate-Gyro-Linear-Accelerometer (RGLA) module

is shown in Fig. 1. The gyros are the Hamilton Standards miniature series 54 Supergyros with $\pm 5,000$ deg/sec dynamic range. These are single-axial rate transducers weighing three ounces each with 1"D x 1.5"L size. Note that these gyros are the standard "off-the-shelf" low cost items. They were purchased with no special requirements other than the dynamic range.

The accelerometers are the commonly used Endevco Model 2264A-2K-R piezoresistive miniature linear accelerometers with $\pm 2,000$ g dynamic range. They are single-axial transducers weighing 1.5 grams each. The size is 0.2" x 0.5" x 0.5". The specified linearity is $\pm 1\%$ of reading and the specified cross-axis coupling is $\pm 1.5\%$ of reading.

RATE TABLE CALIBRATION

Three gyros with demodulators were calibrated on a Genisco rate table at ± 540 deg/sec and $\pm 1,343$ deg/sec angular velocities as illustrated in Fig. 2. The rate table generated a well controlled angular velocity about its spinning axis. Each gyro was tested under six axial orientations at -10, 0, 10, 80, 90, and 100 degrees. The first three orientations indicated the principal axis performance and the last three orientations indicated the cross-axis coupling and axis misalignment. The test results are summarized in Table 1.

Gyro S/N	Conversion Factor Deg/sec/mv	Max. Principal Axis Error, %		Max. Cross-Axis Sensitivity, %
		Of Reading	Of 1343 Deg/sec	
67441	1.907	2.0	3.7	3.0
1999	1.846	3.9	1.6	1.1
67438	1.947	1.7	1.7	5.2

Table 1. Summary of gyro calibration results.

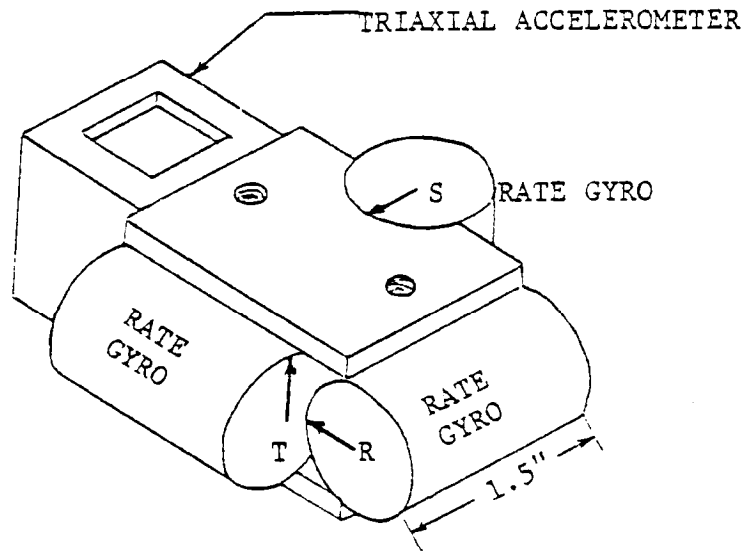


Fig. 1. The Rate-Gyro-Linear-Accelerometer (RGLA) module.

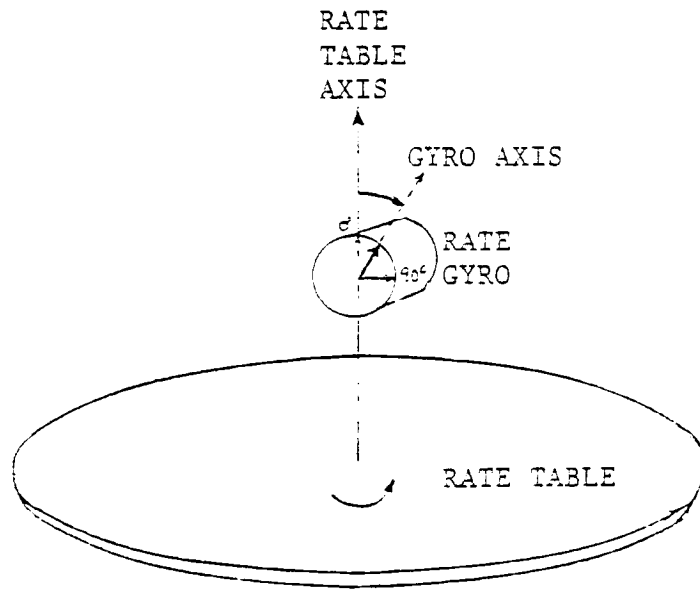


Fig. 2. Rate gyro calibration setup.

PENDULUM TEST: 2-D MODEL

A part 572 50th-percentile male dummy head-neck assembly was attached to a component test pendulum [2] and was released from a 90-degree pendulum angle onto an aluminum honeycomb as shown in Fig. 3. The equivalent pendulum velocity was 19.4 ft/sec. The RGLA module was mounted at the head CG with the instrumentation coordinate R-S-T pitched up 20 degrees from the head anatomical coordinate U-V-W where U was the PA-axis, V was the RL-axis, and W was the IS-axis.

Since the purpose of this experiment was to examine the gyro performance in a planar motion, two identically oriented gyros were used to compare against each other and against the high-speed film data. In other words, three runs were conducted, each with two gyros measuring the same angular velocity about the V-axis. This approximates the angular velocity as seen by the camera looking into the laboratory Y-axis (perpendicular to the pendulum motion plane). Figure 4 shows the three comparisons of the gyro pairs. The linear accelerometer data are shown in Fig. 5.

Figure 6 is the comparison of the gyro data and the film data. Note that the gyro angular velocity was the direct recording from a rate gyro, the angular displacement was integrated from the angular velocity, and the angular acceleration was differentiated from the angular velocity. A five-point least-squares data smoothing process was applied prior to taking the derivative [3]. Data integration was accomplished by using Simpson's 1/3 rule, Newton's 3/8 rule, and a combination of these two rules [3]. Data differentiation was obtained by using the Lagrangian interpolation polynomial of degree 4 relevant to five successive points [3]. The data rate was 1,000 samples/sec.

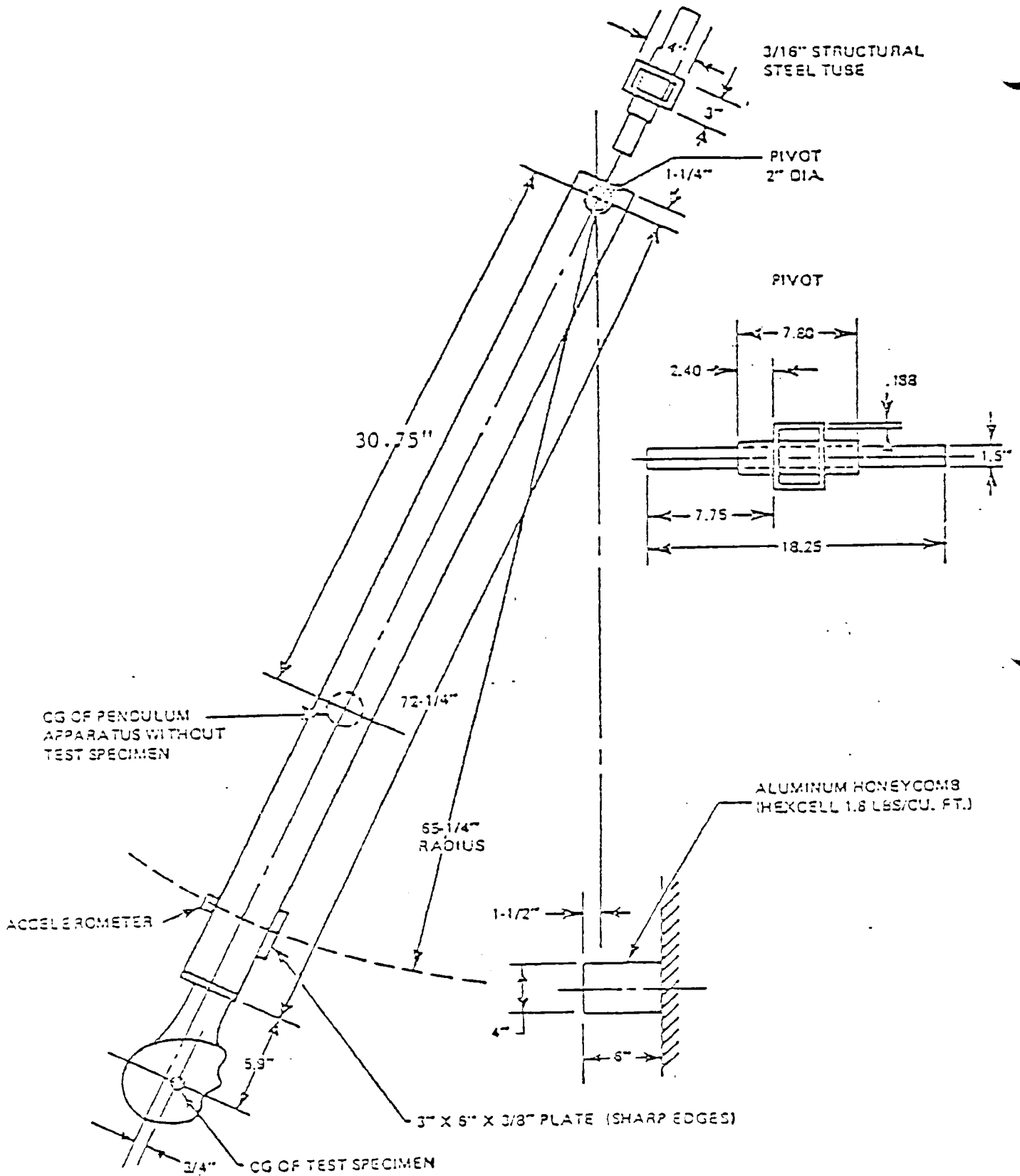
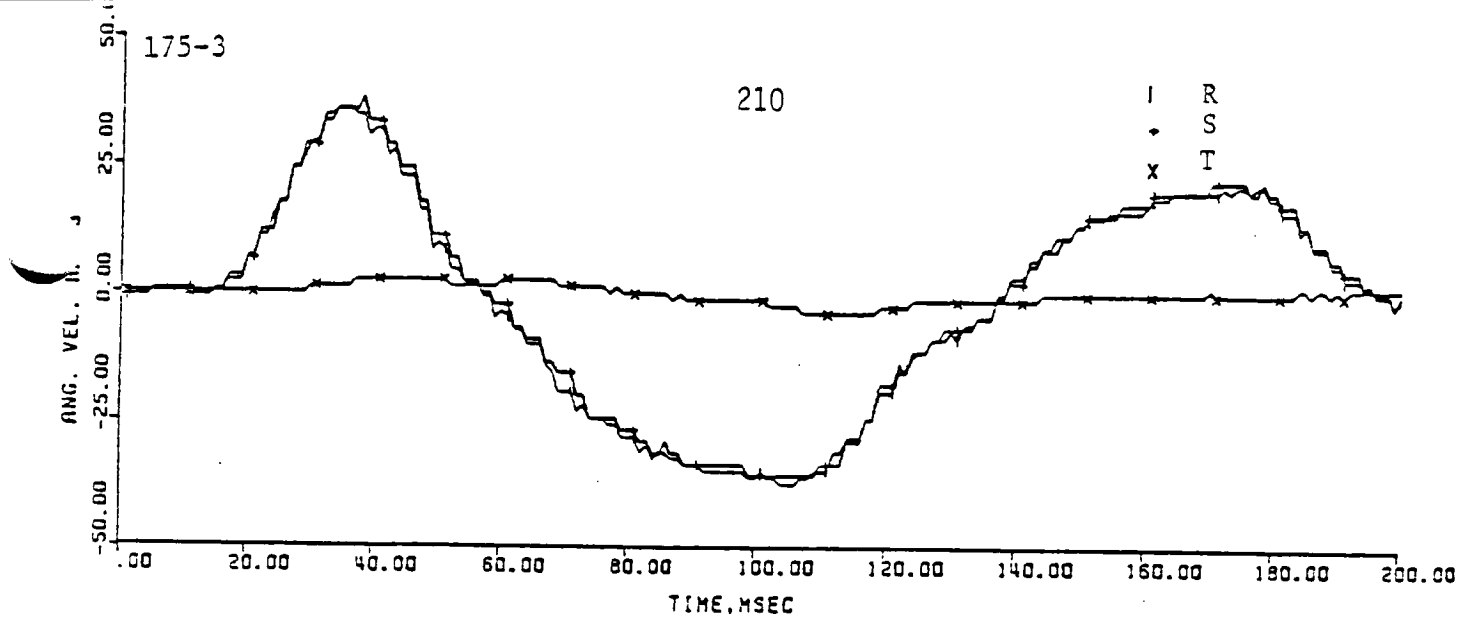
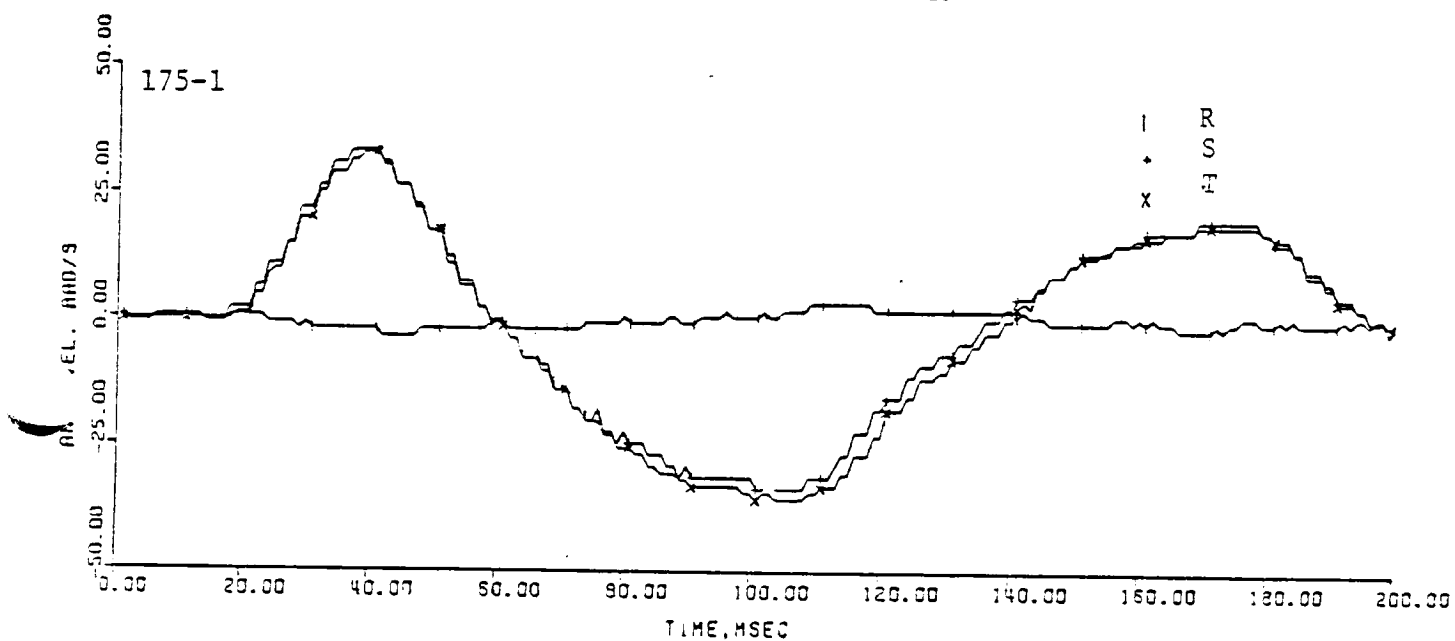


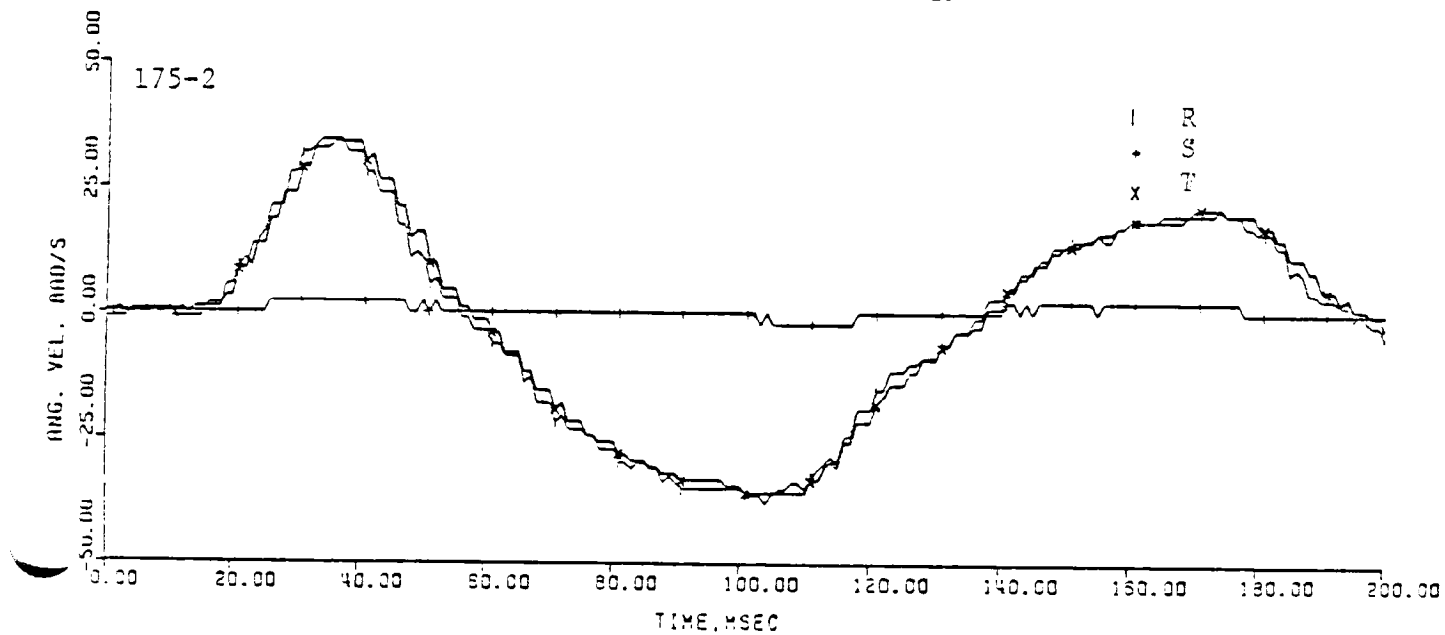
Fig. 3. Head-neck pendulum test setup.



(a) Comparison of R and S gyros.



(b) Comparison of S and T gyros.



(c) Comparison of T and R gyros.

Fig. 4. Comparison of gyro pairs.

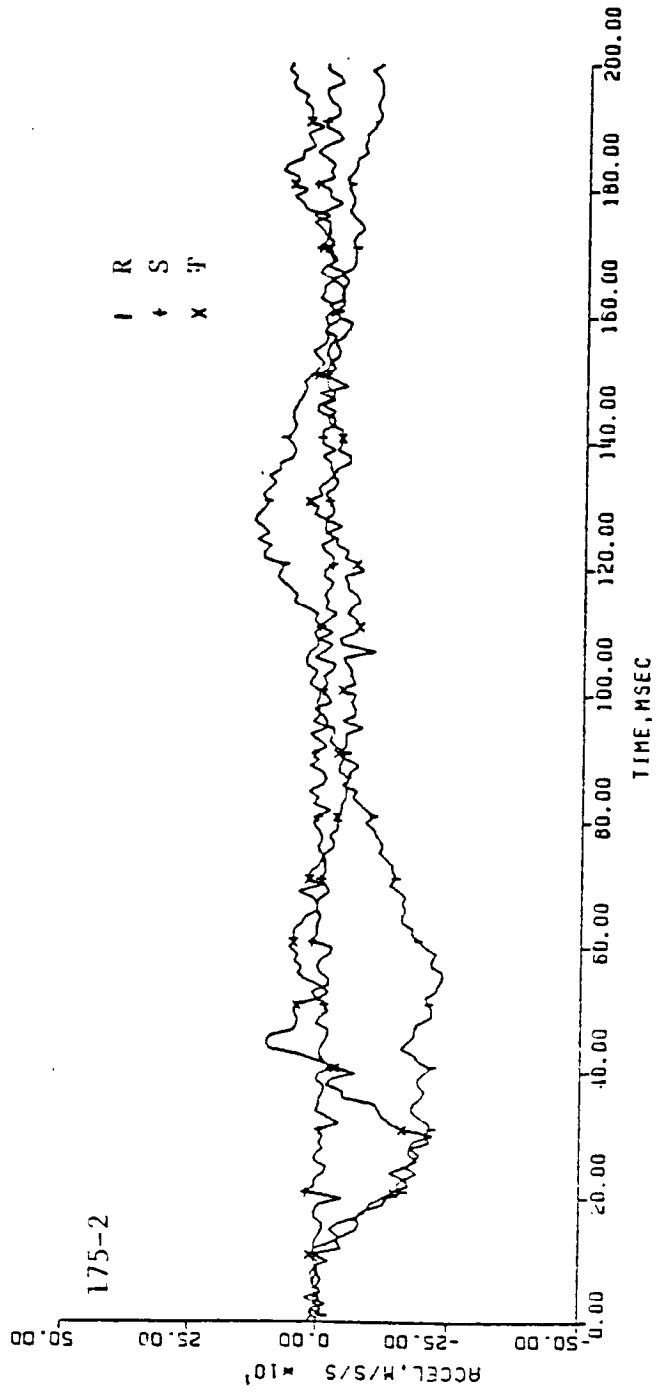
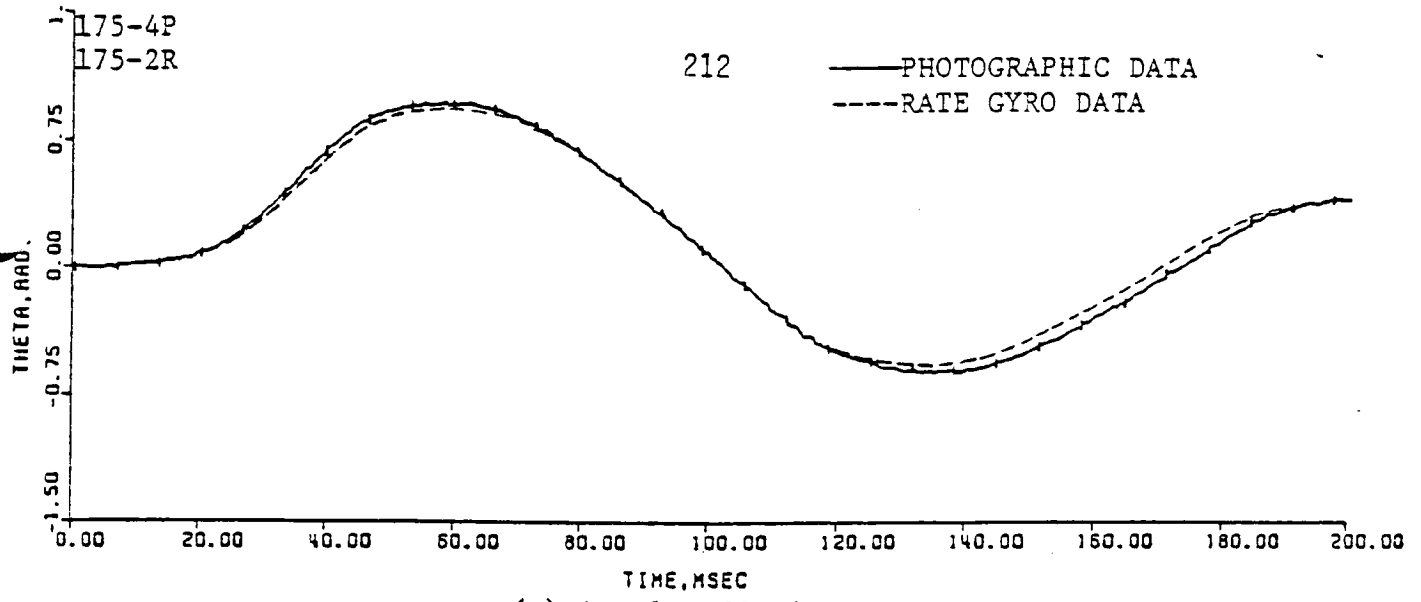
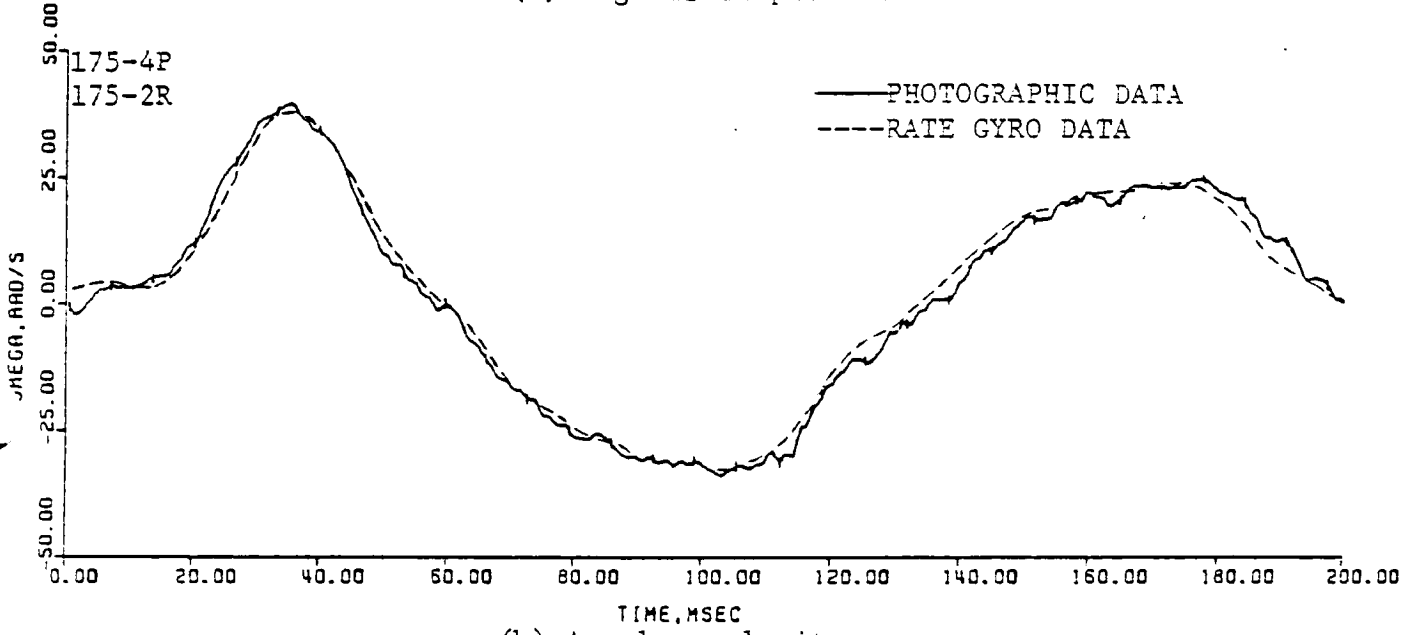


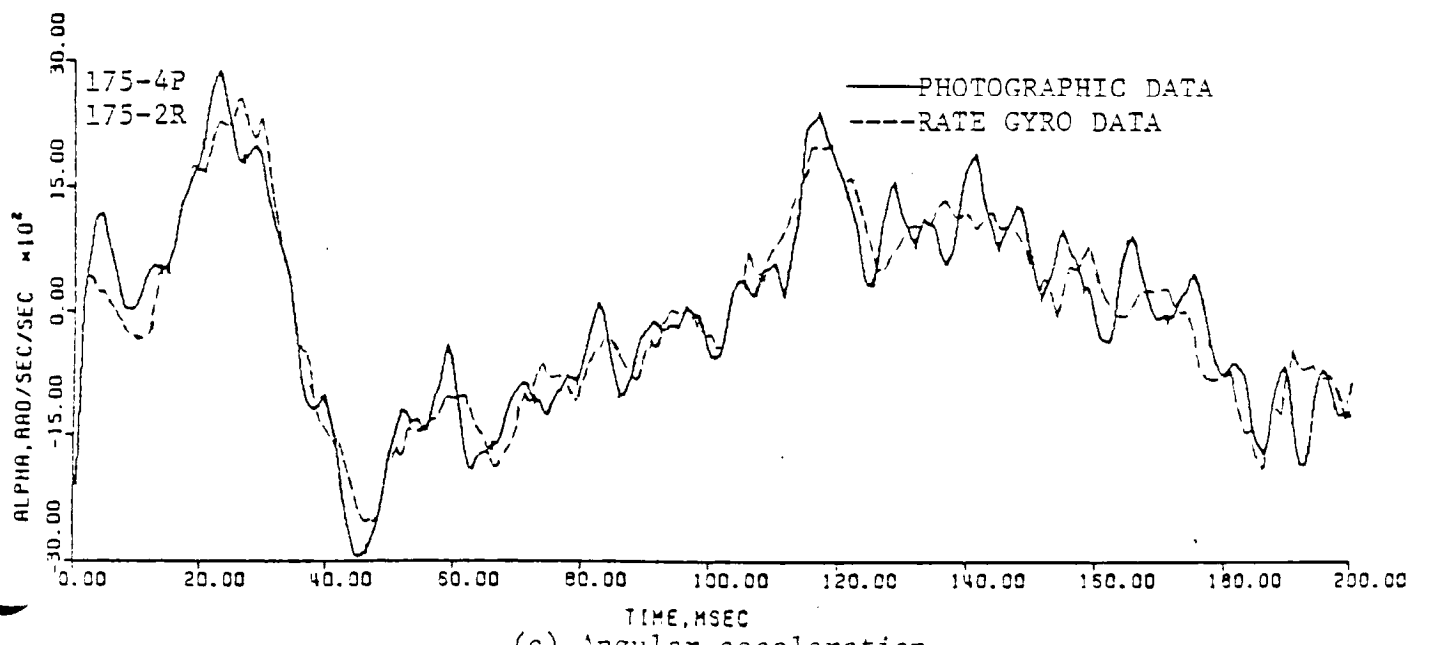
Fig. 5. Linear accelerations, 2-D model.



(a) Angular displacement.



(b) Angular velocity.



(c) Angular acceleration.

Fig. 6. Comparison of rate gyro and film data, 2-D model.

The film angular displacement was the direct film reading, the angular velocity was the first derivative of the angular displacement, and the angular acceleration was the second derivative of the angular displacement. Again, the data smoothing process was applied prior to each differentiation process. The sampling (frame) rate was 1,500 samples/sec.

The agreement between these two methods validates the application of rate gyros in planar motion.

FREQUENCY RESPONSE AND DIFFERENTIATION REQUIREMENTS

In order to compare the gyro data with the film data, integrations and differentiations were used. Integration and differentiation, when considered in frequency domain, are low- and high-pass filtering processes where the frequency harmonics (components) are weighted at -6 dB/octave and $+6$ dB/octave respectively. Therefore, an acceleration measurement requires higher frequency response than a velocity measurement. A velocity measurement, in turn, requires higher frequency response than a displacement measurement. Although integrations and differentiations can be applied quite freely to the measurements, they have drawbacks. For example, a single integration accumulates bias error proportional to time and a double integration accumulates bias error proportional to time-squared. On the other hand, a differentiation removes the bias error but amplifies the high frequency noise associated with the measurement.

This section discusses the frequency response requirements for measurement data which are subjected to the processes of integration and differentiation.

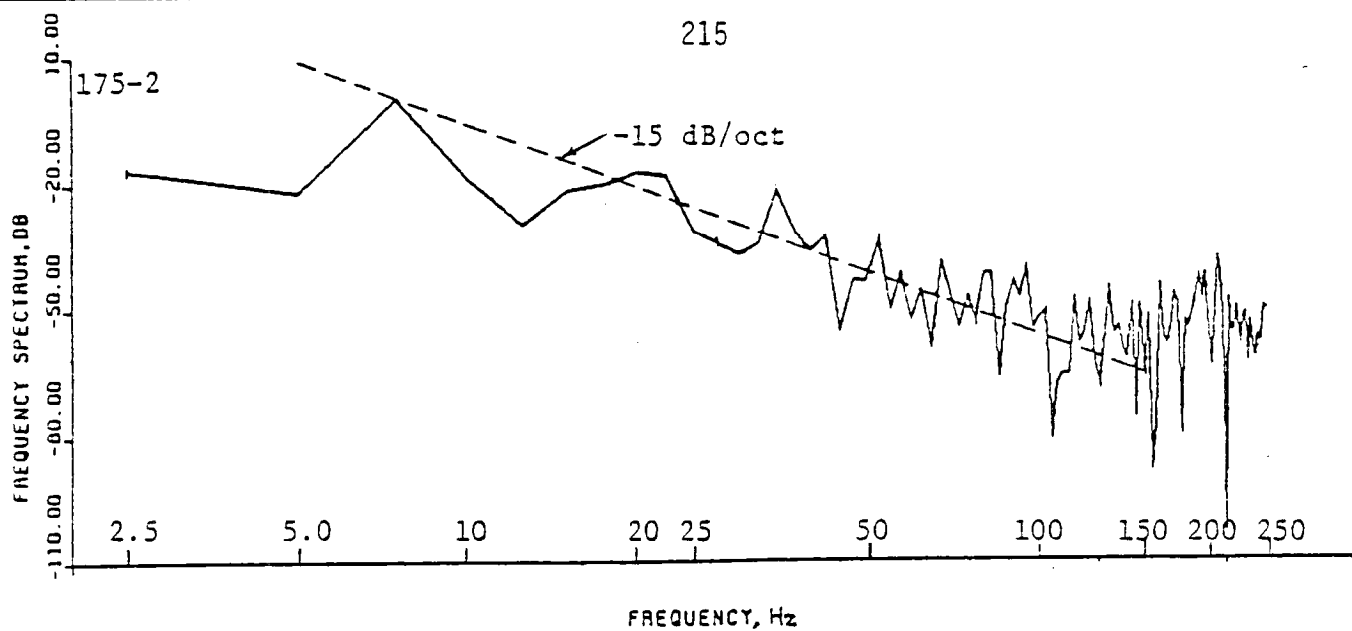
This allows compatible kinematic comparisons between the gyro and the film data. Furthermore, since the frequency response requirement becomes more stringent only when taking derivatives, this section presents only the differentiation requirements.

Gyro Data

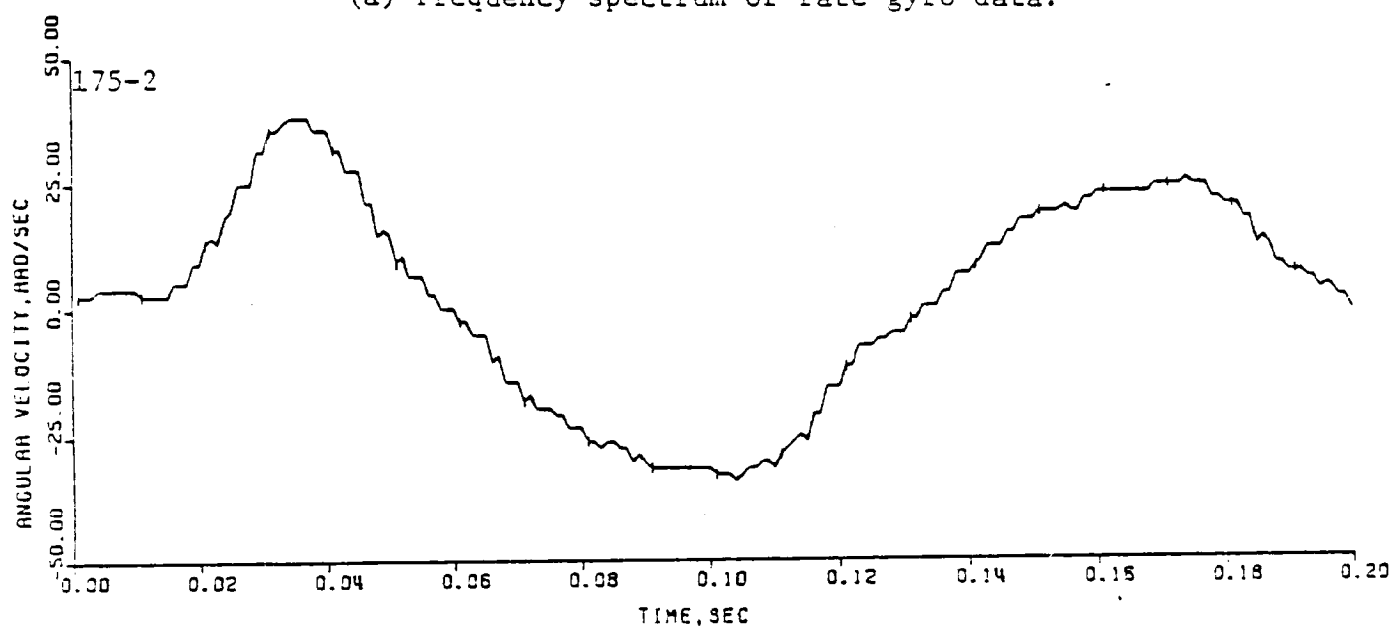
Figure 7a is the frequency spectrum of the raw rate gyro (angular velocity) data of Fig. 7b. It appears that the significant frequency components are below 100 Hz (40th harmonic of the fundamental frequency of 2.5 Hz). Using 60 harmonics (150 Hz) the angular velocity was reconstructed using a truncated Fourier series as shown Fig. 7c. This curve is essentially identical to the curve in Fig. 7b except the high frequency fluctuations had been removed. This verifies that the gyro data do not contain significant angular velocity information above 150 Hz. (The gyro has a natural frequency of 360 Hz with a damping ratio of 0.7.)

The angular displacement (Fig. 6a), obtained by integrating the curve of Fig. 6b, has very little information loss by using only 150 Hz bandwidth. This is because angular displacement requires lower bandwidth than does angular velocity.

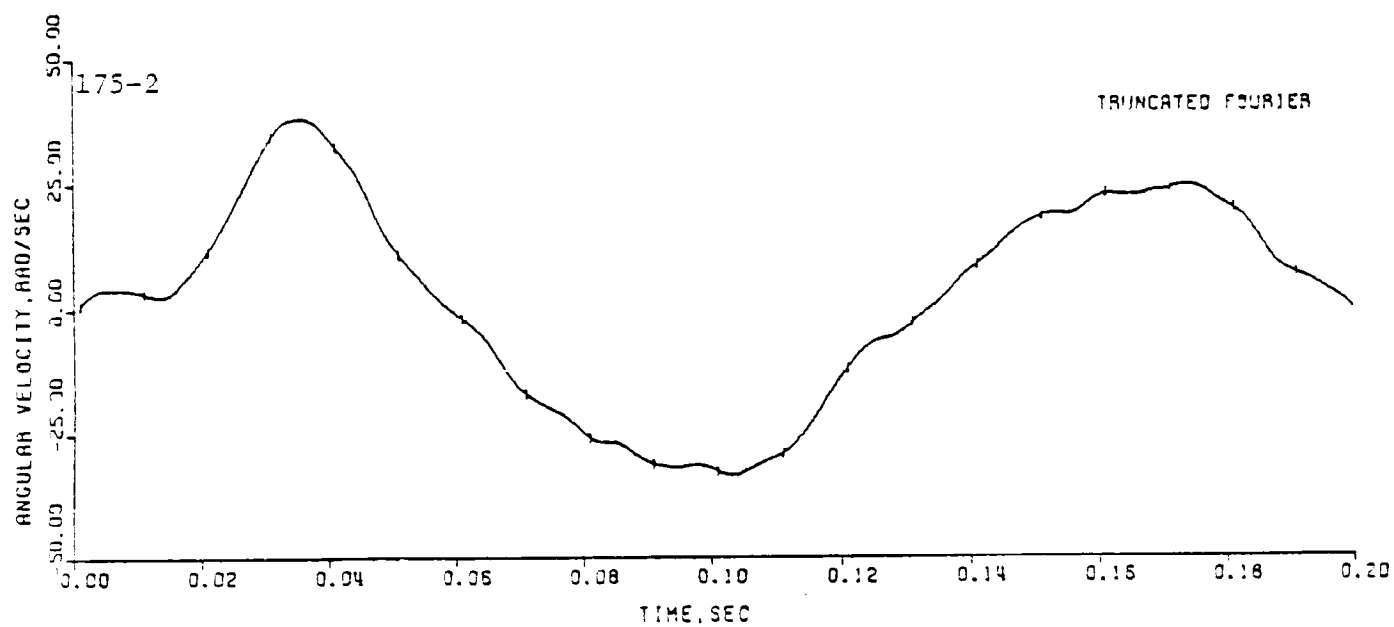
Figure 8 shows the angular accelerations obtained by using three differentiation methods: the Lagrangian polynomial method [3], the truncated Fourier series method [4] and the Lanczos convergence factor method [4], [5]. A five-point smoothing process was applied prior to using the first method. The last two methods were applied for 60 harmonics (150 Hz cutoff frequency). The first



(a) Frequency spectrum of rate gyro data.

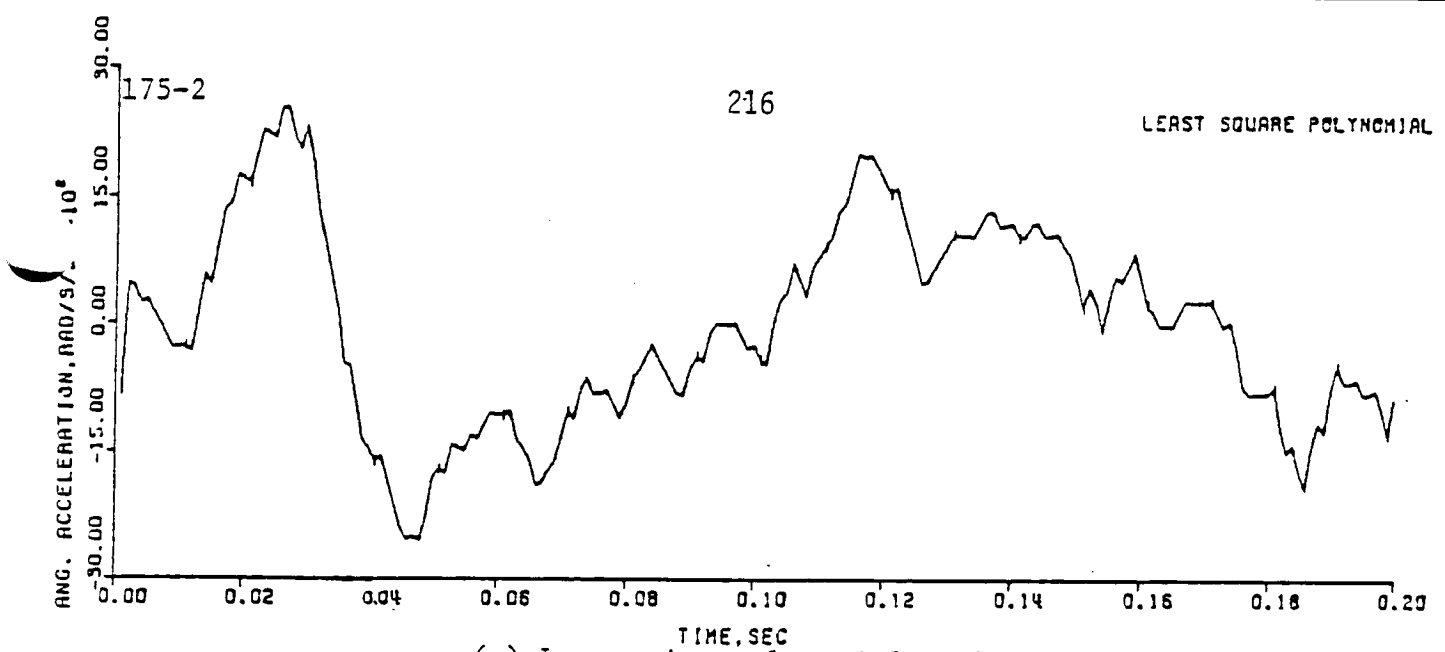


(b) Rate gyro data.

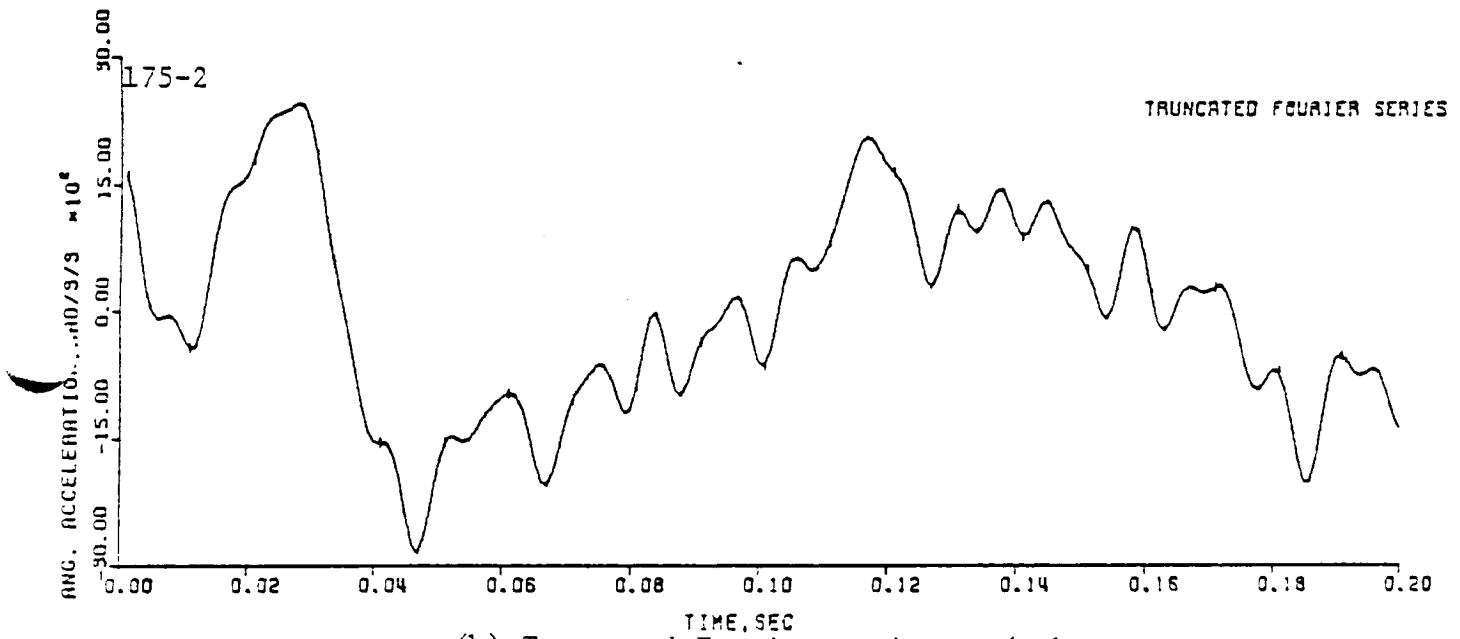


(c) Reconstructed rate gyro data.

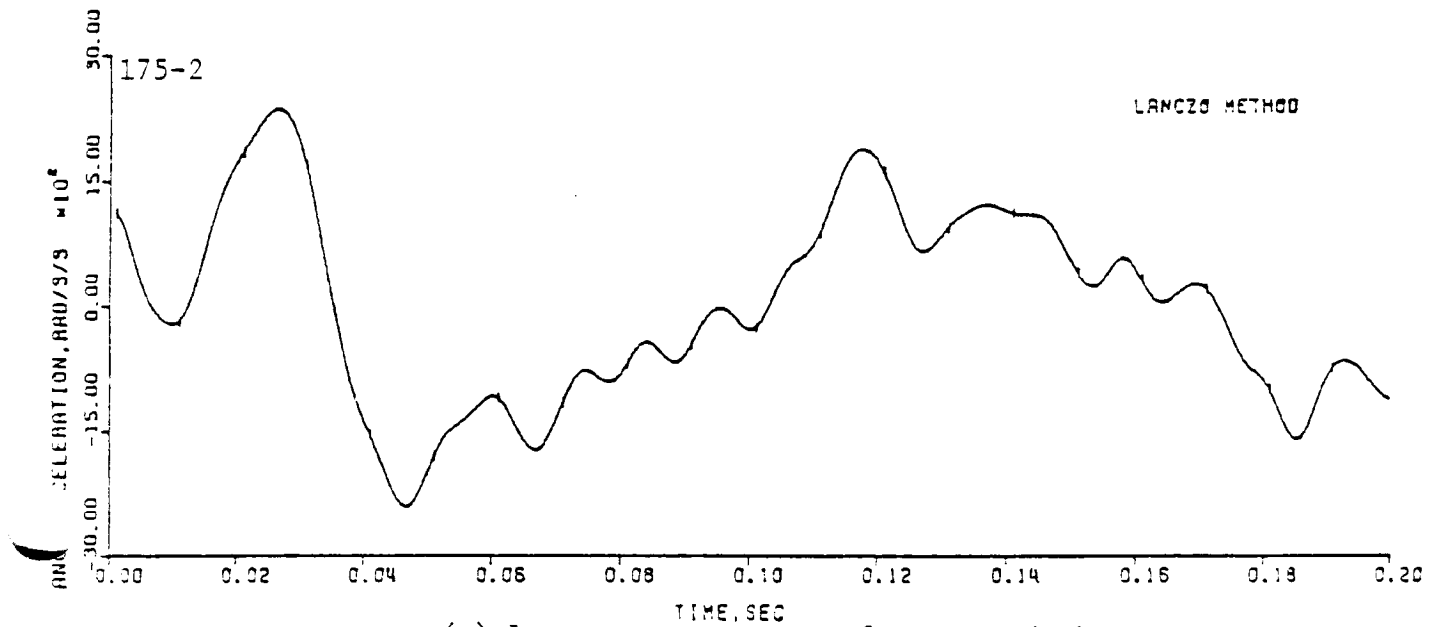
Fig. 7. Rate gyro data and frequency spectrum.



(a) Lagrangian polynomial method.



(b) Truncated Fourier series method.



(c) Lanczos convergence factor method.

Fig. 8. Angular acceleration, rate gyro data.

method operates in the time domain while the last two methods operate in the frequency domain. These first derivatives are nearly identical except the high-frequency components.

Film Data

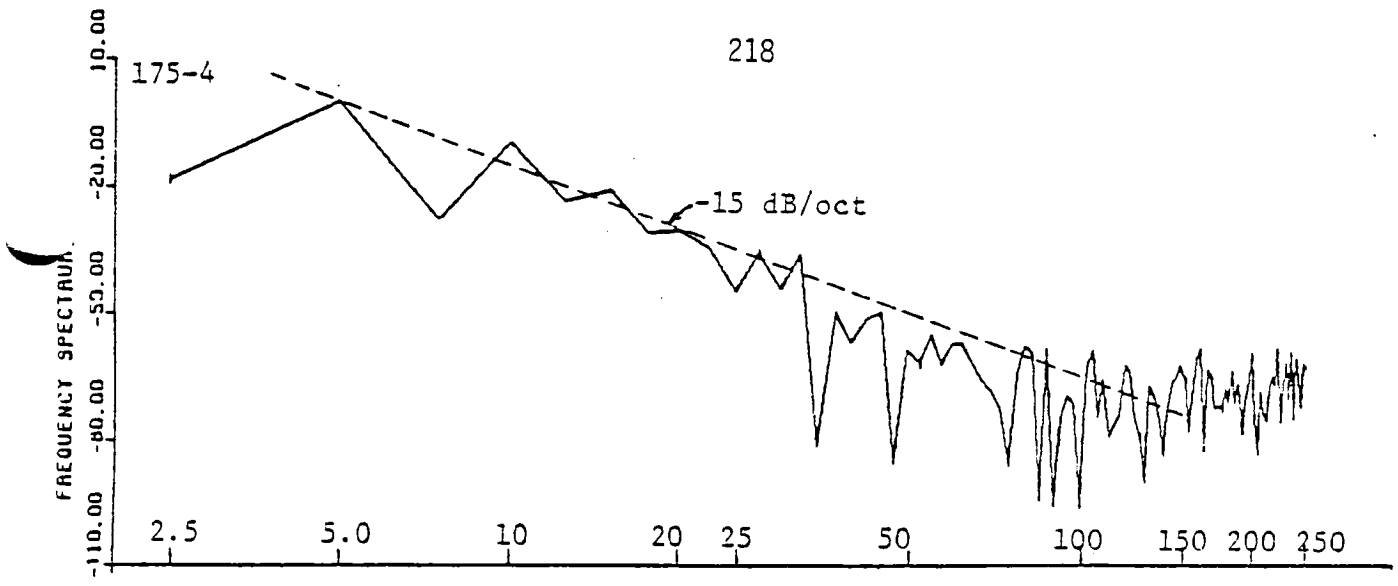
Figure 9a is the frequency spectrum of the raw film (angular displacement) data of Fig. 9b. Using the same -15 dB/octive asymptote of Fig. 7a as a reference, it becomes apparent that the angular displacement spectrum drops off at a more rapid rate than does the angular velocity spectrum. This is expected because angular velocity is the derivative of angular displacement. It also appears that the significant frequency components are below 50Hz. Figure 9c is the reconstructed angular displacement using a truncated Fourier series of 60 harmonics. The film data sampling rate was 1,500 samples/sec.

Again, the same three methods were used to take the first derivative (angular velocity, Fig. 10) and the second derivative (angular acceleration, Fig. 11). A five-point smoothing process was applied prior to taking each derivative for the Lagrangian polynomial method. The cutoff frequency was 150 Hz for both the truncated Fourier series and the Lanczos convergence factor methods.

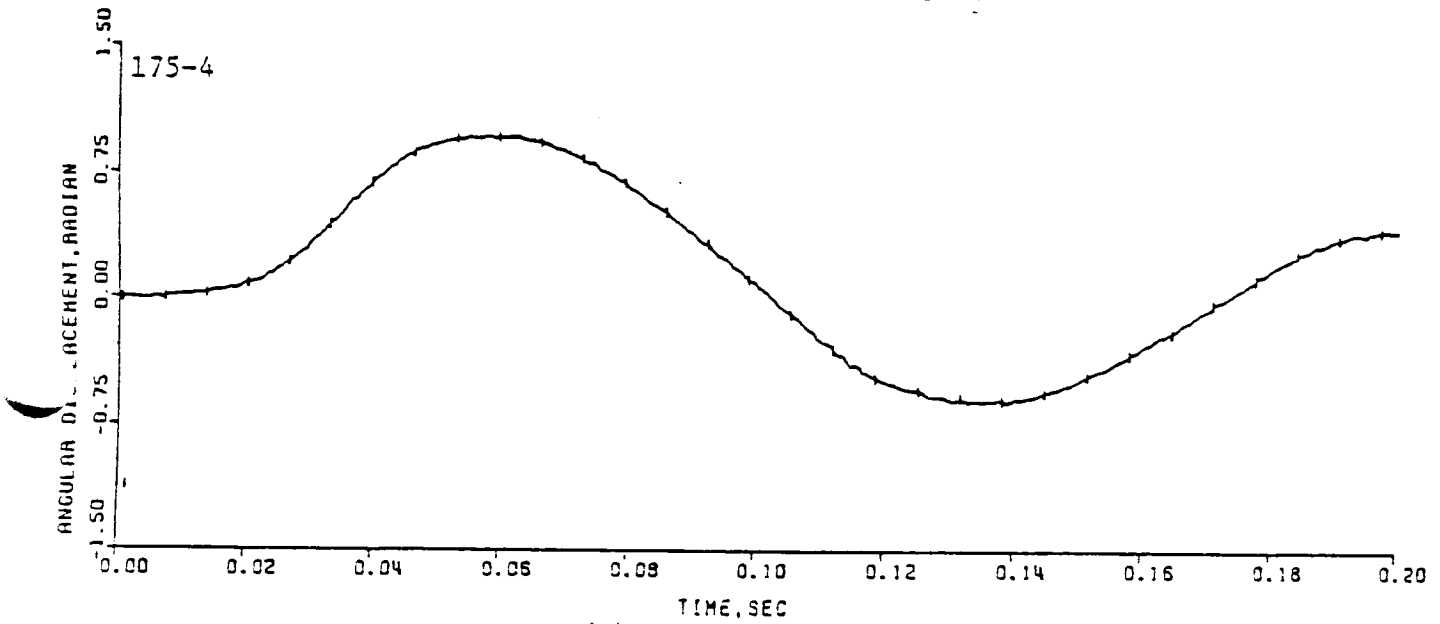
It appears, at least in Fig. 11, that the results of the first two methods are nearly identical except the high-frequency components. The last method, even with 60 harmonics, has severe low-pass filtering effect.

Discussions

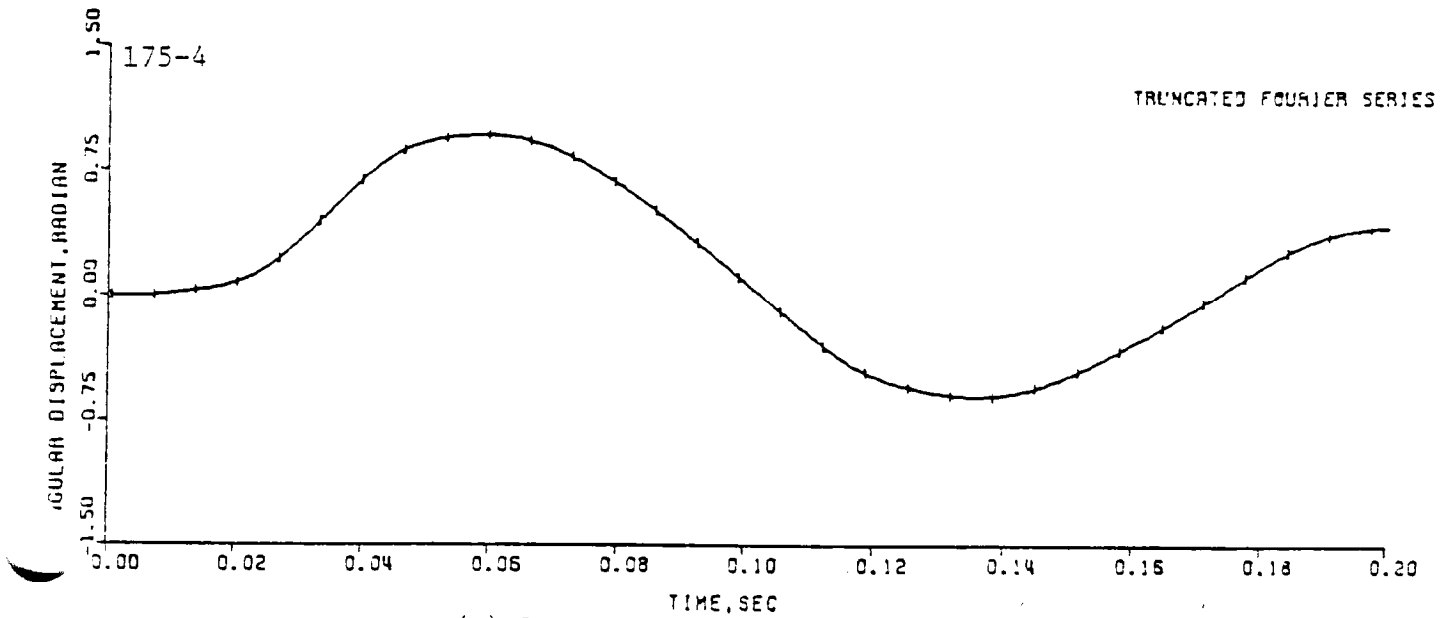
This section discussed the importance of the harmonic analysis in esta-



(a) Frequency spectrum of photographic data.

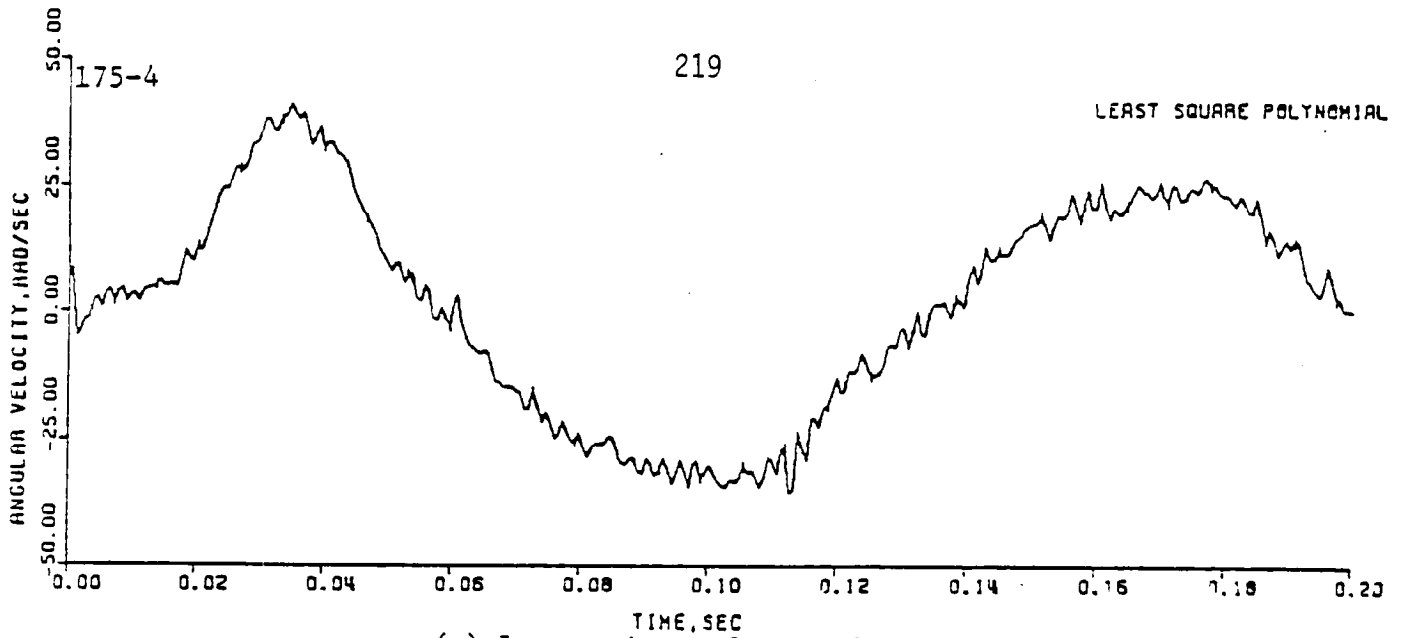


(b) Photographic data.

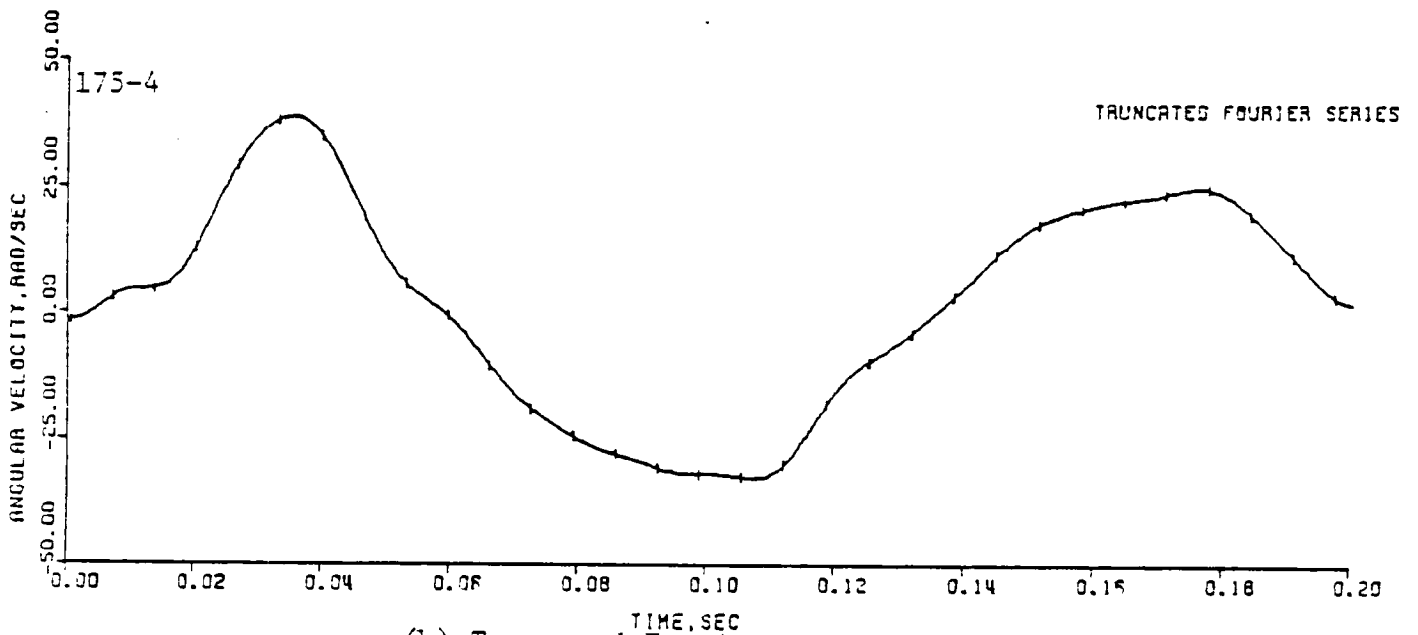


(c) Reconstructed photographic data.

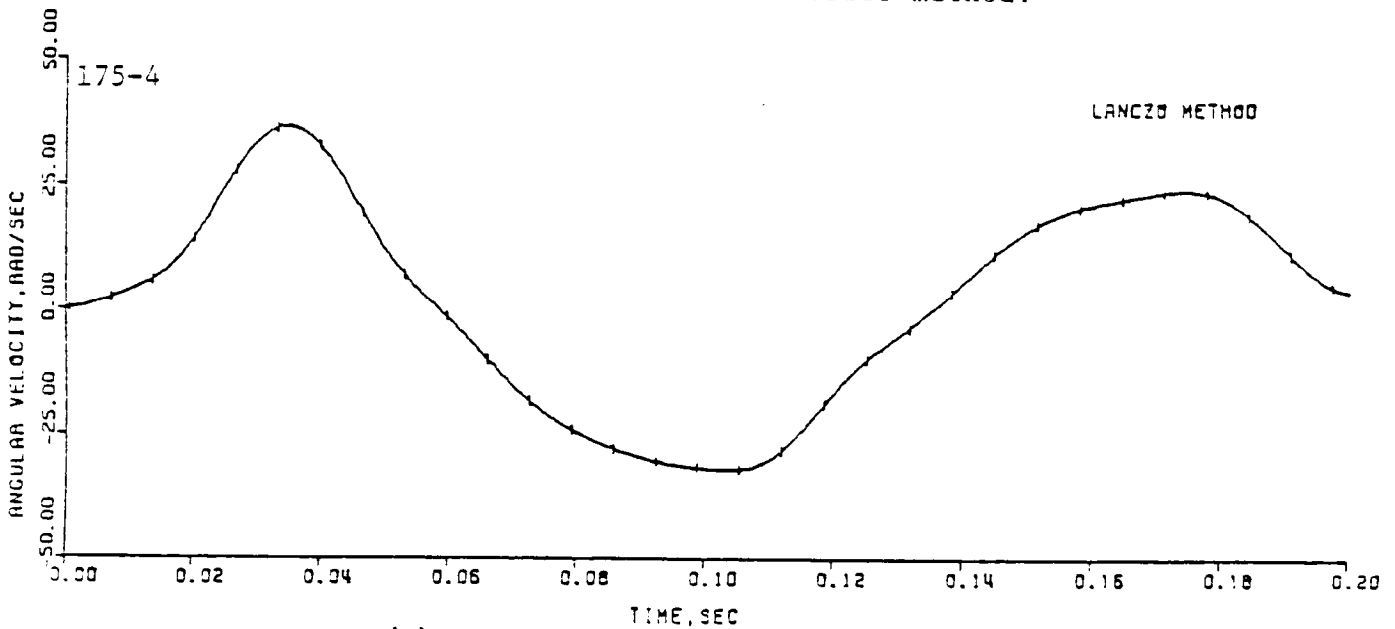
Fig. 9. Film data and frequency spectrum.



(a) Lagrangian polynomial method.

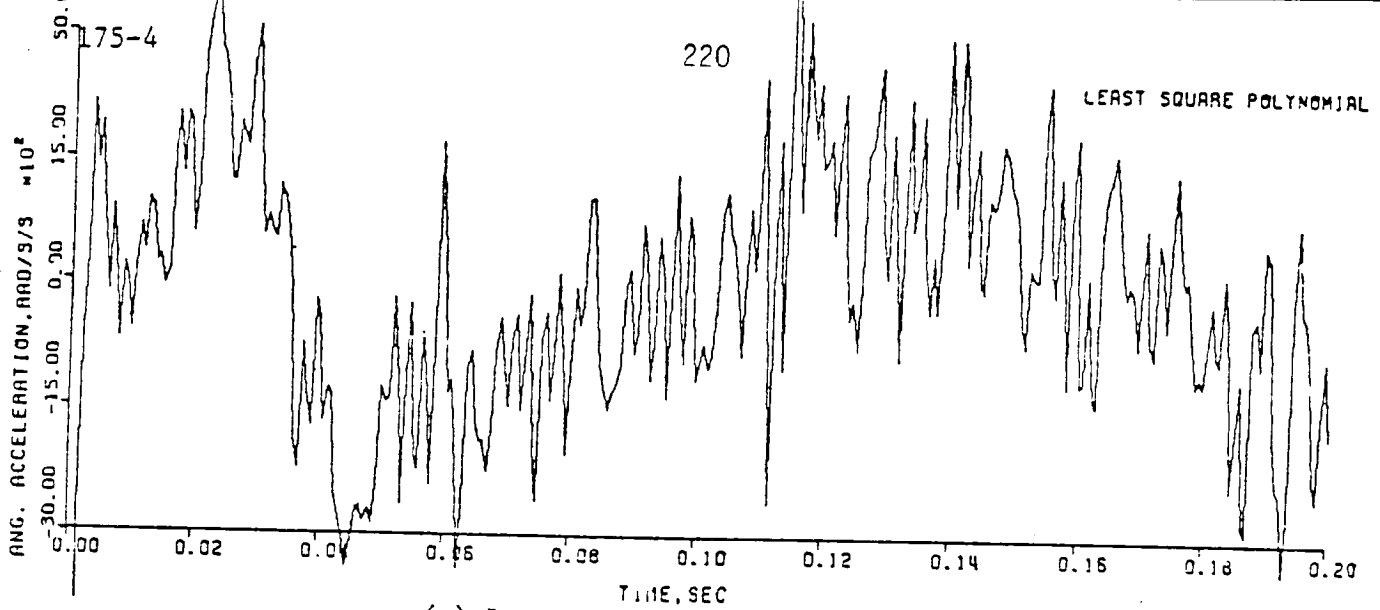


(b) Truncated Fourier series method.

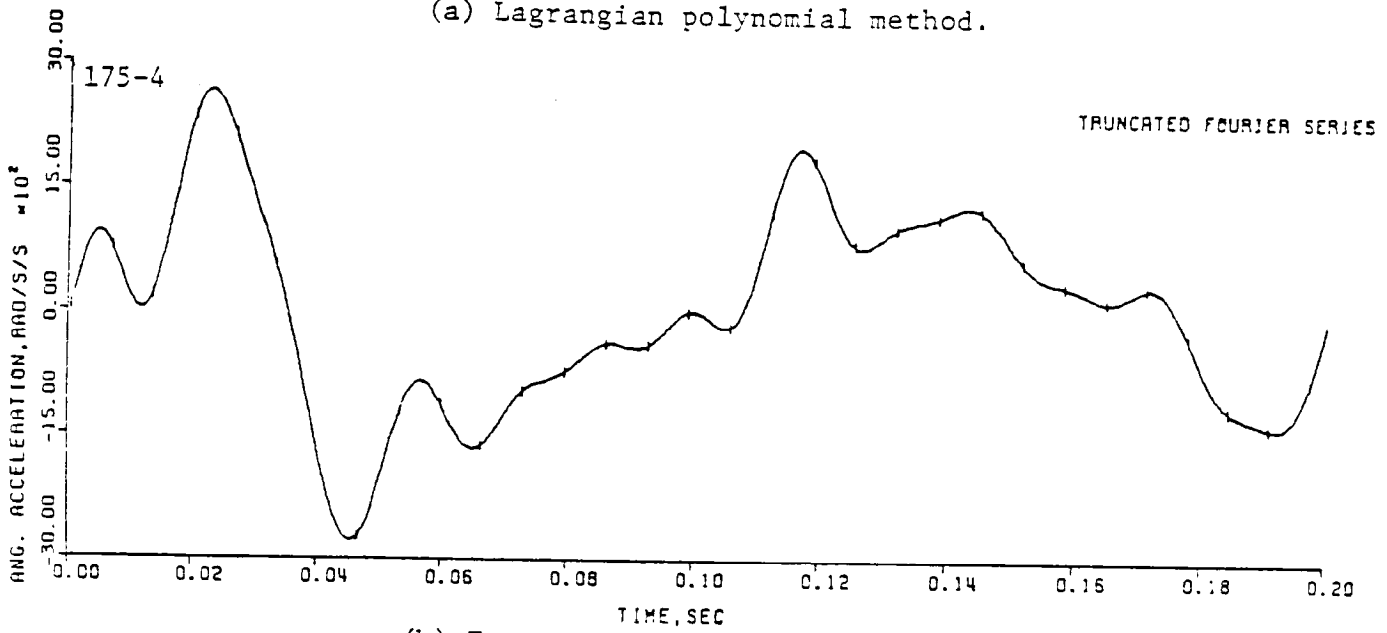


(c) Lanczos convergence factor method.

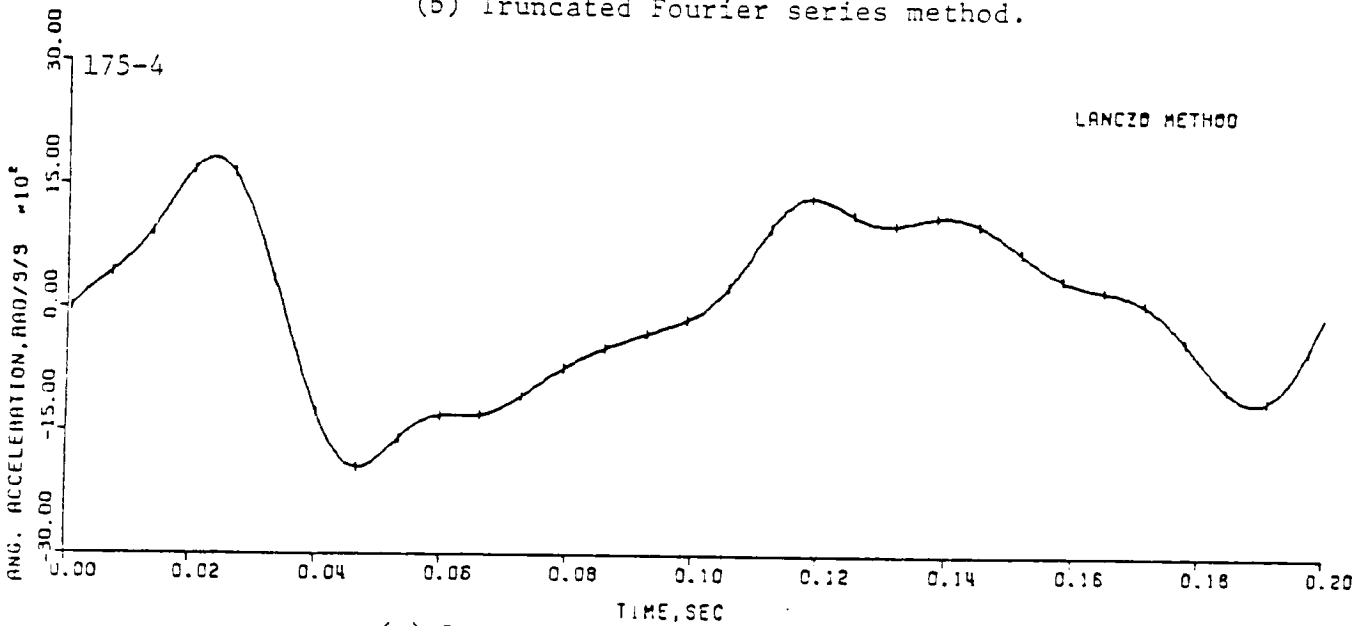
Fig. 10. Angular velocity, film data.



(a) Lagrangian polynomial method.



(b) Truncated Fourier series method.



(c) Lanczos convergence factor method.

Fig. 11. Angular acceleration, film data.

blishing the data channel frequency response and sampling rate requirements. Three commonly used differentiation methods, i.e., the Lagrangian polynomial, the truncated Fourier series, and the Lanczos convergence factors were demonstrated.

From this and other studies [5], [6], it can be concluded that the selection of the total number of harmonics used in the last two differentiation methods must be higher than that used to reconstruct the function itself. A 6 dB/octive for the first derivative and a 12 dB/octive for the second derivative high-pass equivalent effect must be taken into consideration. The total number of harmonics is limited by the data measurement error and the computational error. Since the rate gyro data and the film data do not contain information above 100 Hz, differentiations using sample rate of 1 KHz are adequate.

The first method is independent of the selection of the harmonics because it operates in time-domain. In general, it is superior to the other two methods as long as the sampling rate is high as compared to the highest frequency component of the function. Unless stated otherwise, all the derivatives presented in this paper were differentiated using this method.

PENDULUM TEST: 3-D MODEL

This experiment used the same pendulum setup as shown in Fig. 3, except that the instrument module was rotated (20 degrees pitch up and 45 degrees yaw right) from the anatomical coordinate. By virtue of this arrangement, a planar motion was able to provide a 3-D kinematic model analysis and to provide easy film data comparison. Figure 12 shows this test setup where R-S-T is the instrumentation coordinate, U-V-W is the anatomical coordinate, and X-Y-Z

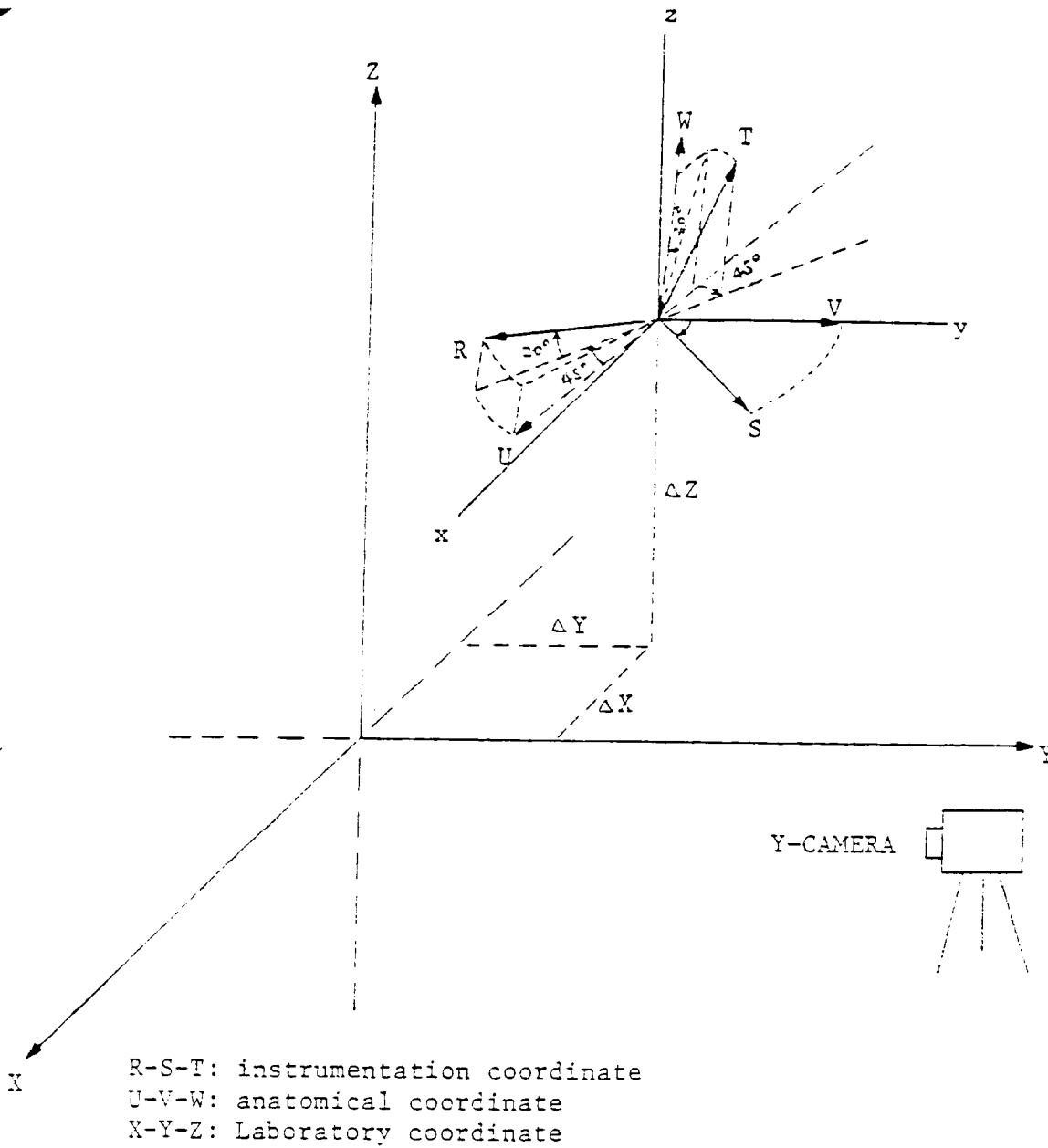


Fig. 12. Pendulum test setup, 3-D model.

is the laboratory coordinate. The raw transducer data are shown in Fig. 13.

Resultant Gyro Data

A quick-look of the gyro data accuracy is to calculate their resultant and compare this resultant with the film data. The advantage of this checking is that the resultant is not directionally dependent. In other words, it retains its value even if the gyros are misaligned. The disadvantage is that the square-root-sum does not provide the changing of sign of the resultant, and this sign must be manually inserted.

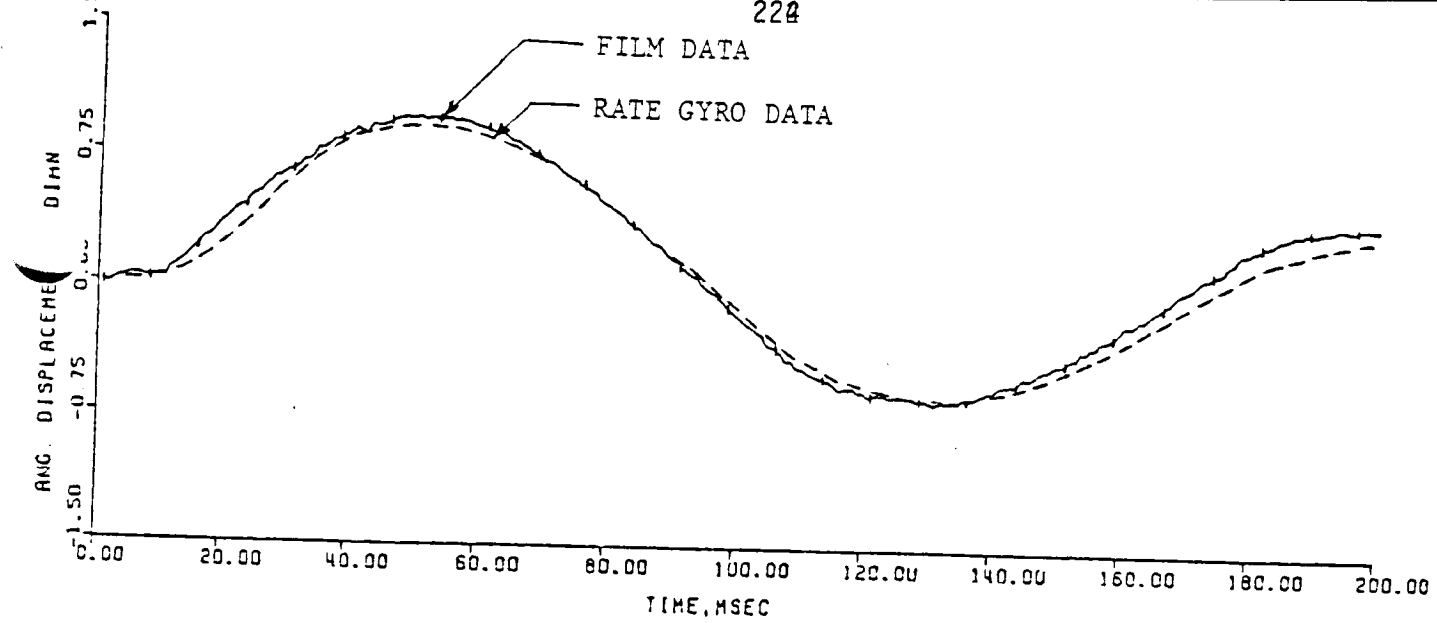
Figure 14 shows both the rate gyro data and the film data where the gyro angular velocity data between 49 and 136 milliseconds had been "assigned" negative. A 5-point least-squares data smoothing process was applied once prior to taking the derivative of the gyro data. For the side view (y-axis) film data, the smoothing process was applied twice prior to each differentiation process.

Anatomical Coordinate Data

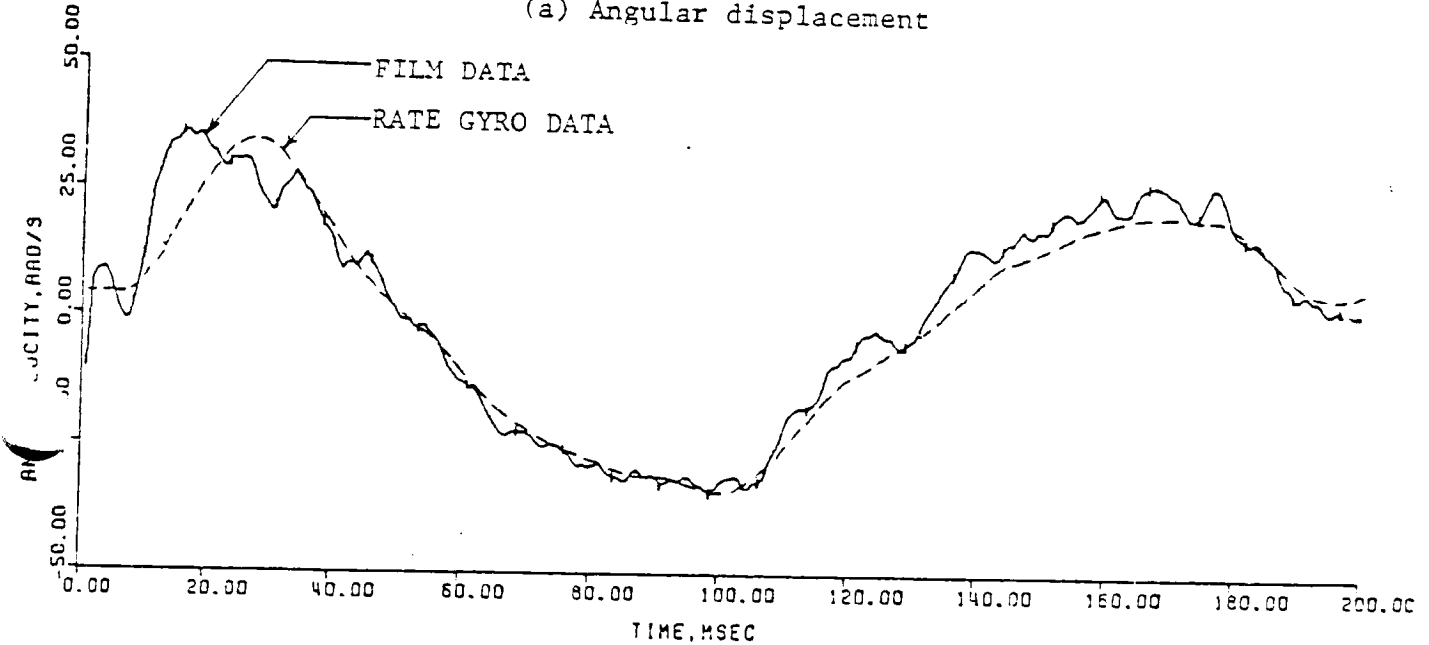
Since the module was located at the head CG, the data transformation from the instrumentation coordinate R-S-T into the anatomical coordinate U-V-W is a simple operation using the following equation.

$$\begin{bmatrix} U \\ V \\ W \end{bmatrix} = \begin{bmatrix} 0.664463024 & 0.707106781 & -0.241844763 \\ -0.664463024 & 0.707106781 & 0.241844763 \\ 0.342020143 & 0 & 0.939692621 \end{bmatrix} \begin{bmatrix} R \\ S \\ T \end{bmatrix}$$

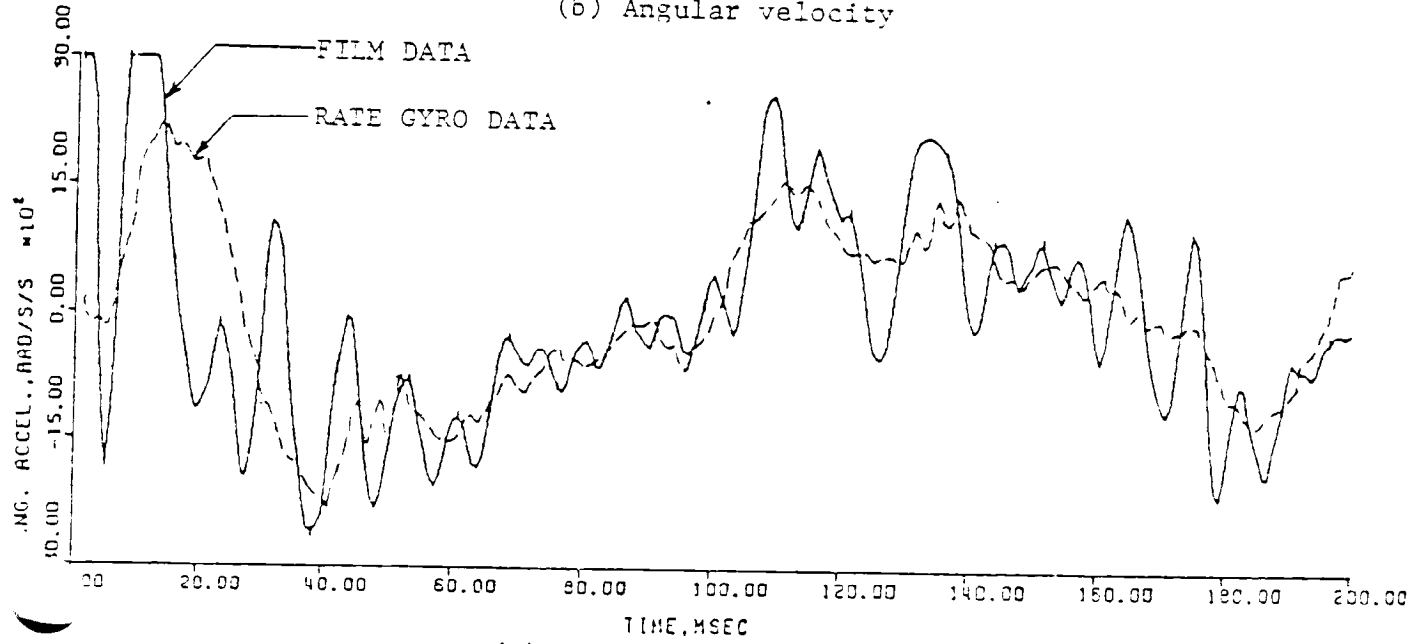
Figure 15 shows the U-V-W components of the transducer data where the dashed curve is the Y-component obtained by film measurement.



(a) Angular displacement

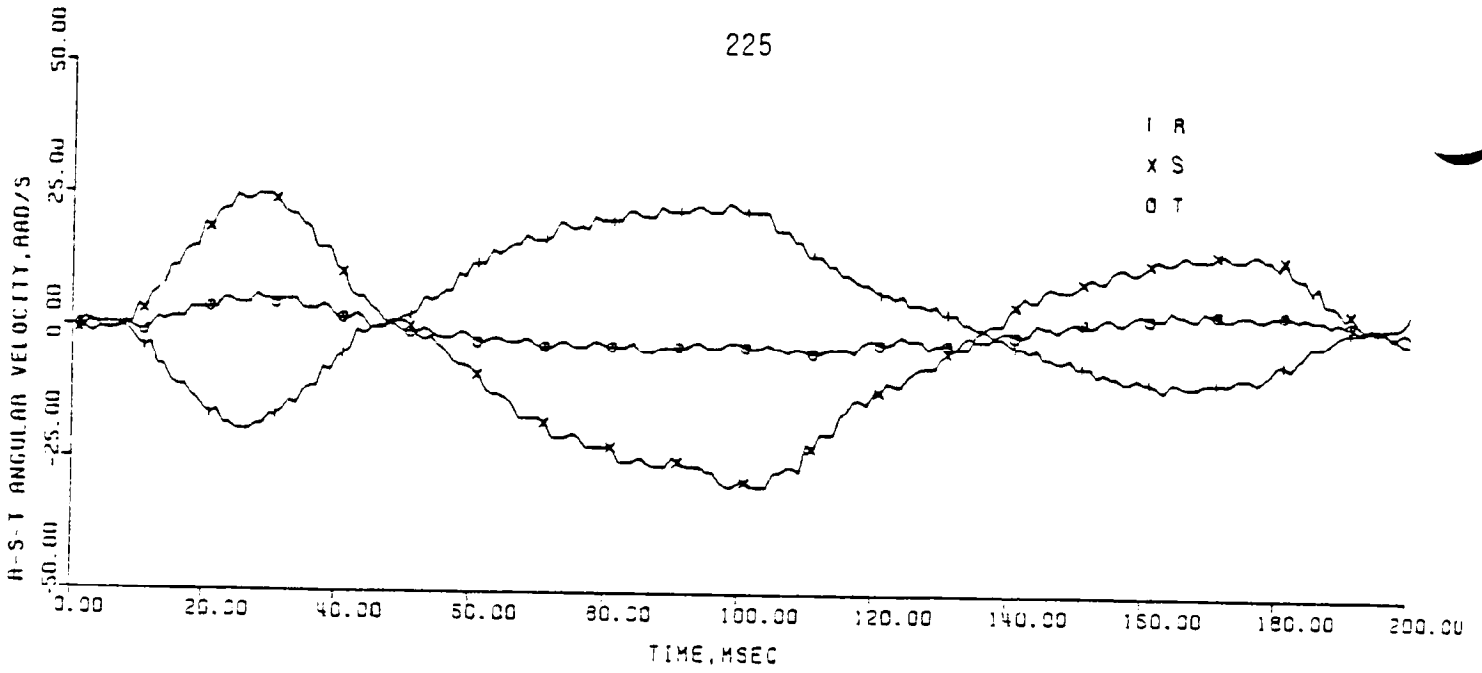


(b) Angular velocity

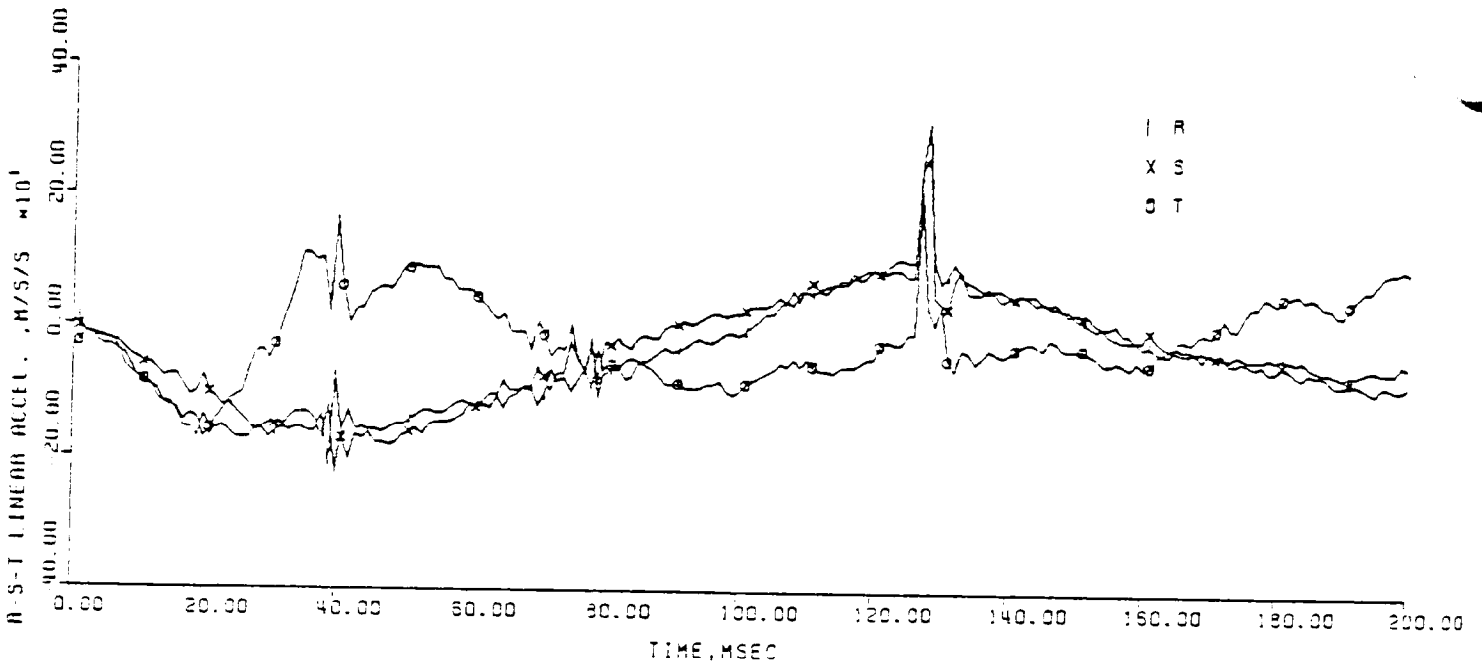


(c) Angular acceleration

Fig. 14. Comparison of resultant rate gyro and film data, 3-D model.

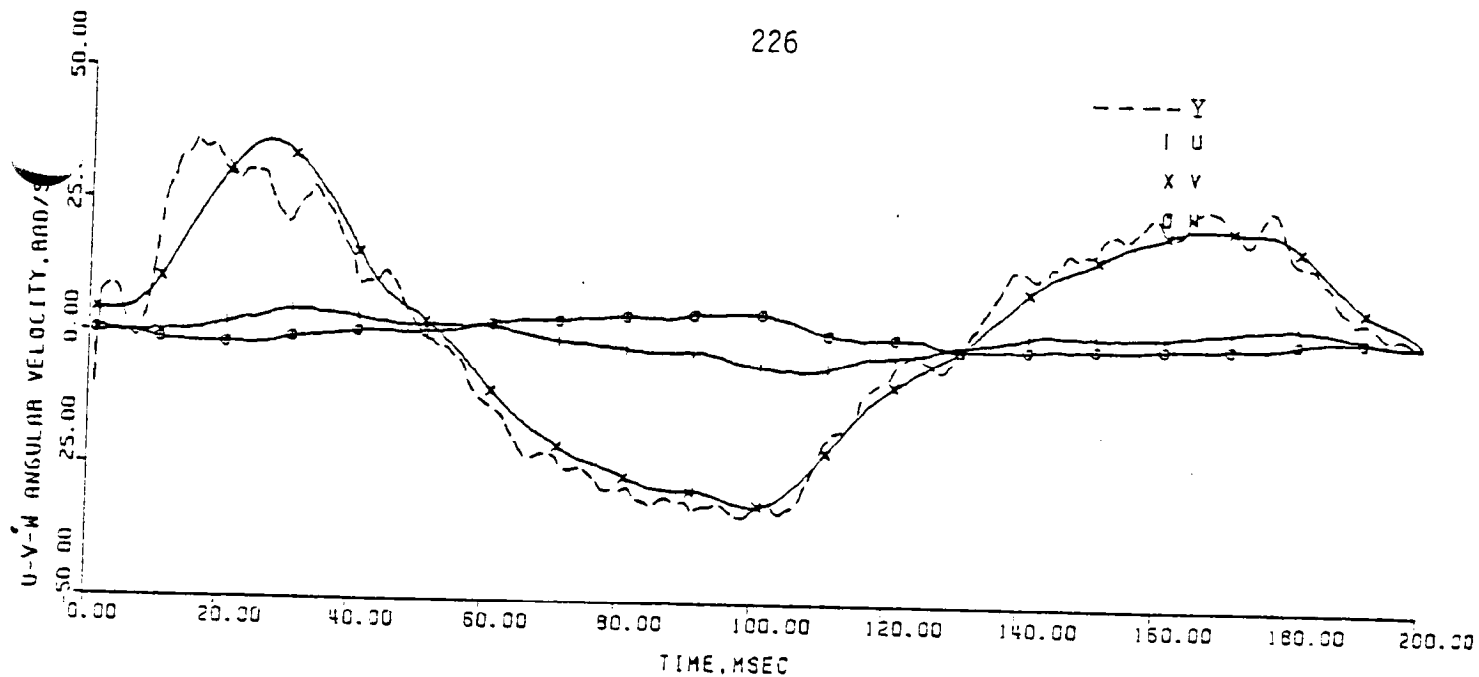


(a) Rate gyro data

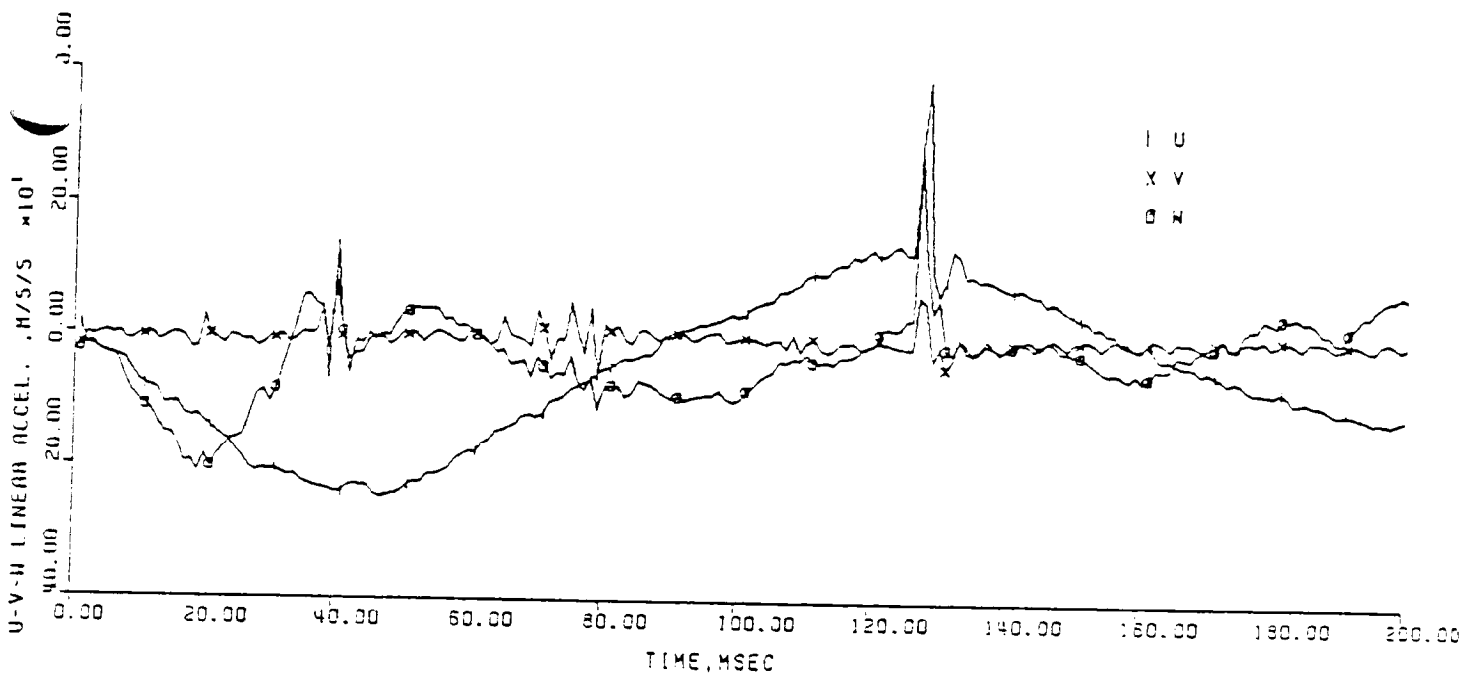


(b) Linear accelerometer data

Fig. 13. Transducer data in instrumentation coordinate.



(a) Rate gyro data



(b) Linear accelerometer data

Fig. 15. Transducer data in anatomical coordinate.

Coordinate Transformation

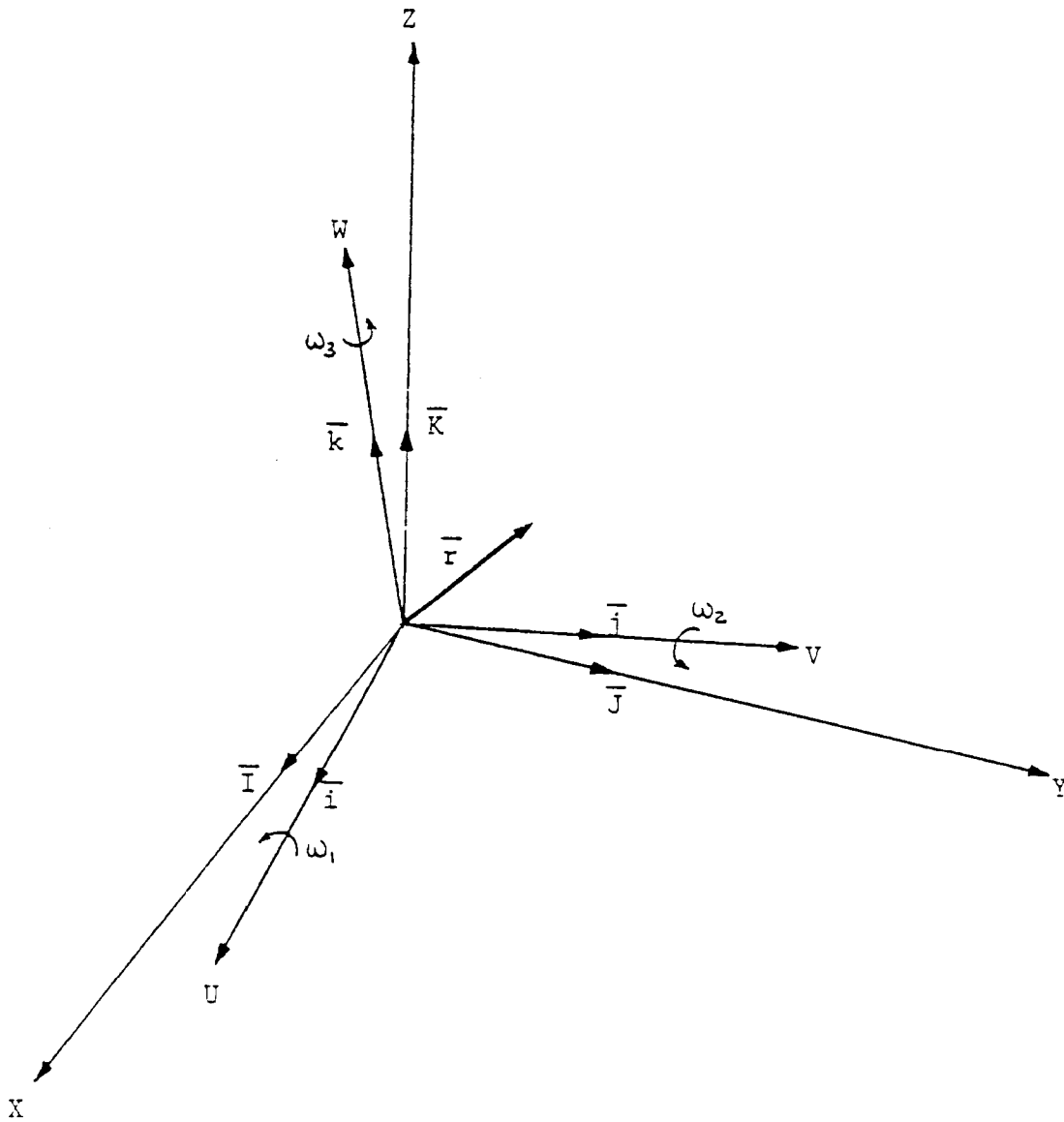
In order to relate the measured electronic data with the film data, the anatomical coordinate (U-V-W) data must be transformed into the laboratory coordinate (X-Y-Z) data. There are several methods for coordinate transformation. Most of them, the yaw-pitch-roll and the Euler angle methods for example, contain the sums and differences of the products of trigonometric functions of angular displacement (integrated from angular velocity) data for computations. This makes the transformation accuracy vulnerable to the measurement errors. The purpose of this section is to derive a rotational transformation method using only the rate gyro measured angular velocity data.*

Let $\bar{i}, \bar{j}, \bar{k}$ be the unit vectors of the anatomical (moving) cartesian coordinate and $\bar{I}, \bar{J}, \bar{K}$ be the unit vectors of the laboratory (fixed) coordinate as shown in Fig. 16. The time derivative of a vector \bar{r} in the two coordinates is then related by [7]

$$D_F \bar{r} = D_M \bar{r} + \bar{\omega} \times \bar{r} \quad (1)$$

where D_F is the derivative of \bar{r} observed in the fixed coordinate, D_M is the derivative of \bar{r} observed in the moving coordinate, and $\bar{\omega}$ is the angular velocity vector.

* This idea was originally suggested by Arnold K. Johnson of the National Highway Traffic Safety Administration in July 1976.



X-Y-Z: FIXED COORDINATE
 U-V-W: MOVING COORDINATE

Fig. 16. Rotating coordinate systems.

Apply Eq. (1) for $\bar{F} = \bar{I}$, $\bar{F} = \bar{J}$, and $\bar{F} = \bar{K}$. This equation becomes

$$\left[\begin{array}{c} \frac{d\bar{i}(t)}{dt} \\ \frac{d\bar{j}(t)}{dt} \\ \frac{d\bar{k}(t)}{dt} \end{array} \right]_{\bar{F}} = \left[\begin{array}{ccc} 0 & w_3(t_1) & -w_2(t_1) \\ -w_3(t_1) & 0 & w_1(t_1) \\ w_2(t_1) & -w_1(t_1) & 0 \end{array} \right] \left[\begin{array}{c} \bar{i}(t_1) \\ \bar{j}(t_1) \\ \bar{k}(t_1) \end{array} \right] \quad (2)$$

$t=t_1$

These differential equations can be approximated by the difference equations at t_1 as

$$\left[\begin{array}{c} \Delta\bar{i}(t_1) \\ \Delta\bar{j}(t_1) \\ \Delta\bar{k}(t_1) \end{array} \right]_{\bar{F}} = h \left[\begin{array}{ccc} 0 & w_3(t_1) & -w_2(t_1) \\ -w_3(t_1) & 0 & w_1(t_1) \\ w_2(t_1) & -w_1(t_1) & 0 \end{array} \right] \left[\begin{array}{c} \bar{i}(t_1) \\ \bar{j}(t_1) \\ \bar{k}(t_1) \end{array} \right] \quad (3)$$

where h is the time increment.

Initially, at time t_1 , these two coordinates are related by the direction cosine matrix $[\bar{a}_{mn}(t_1)]$.

$$\left[\begin{array}{c} \bar{i}(t_1) \\ \bar{j}(t_1) \\ \bar{k}(t_1) \end{array} \right] = \left[\begin{array}{ccc} a_{11}(t_1) & a_{12}(t_1) & a_{13}(t_1) \\ a_{21}(t_1) & a_{22}(t_1) & a_{23}(t_1) \\ a_{31}(t_1) & a_{32}(t_1) & a_{33}(t_1) \end{array} \right] \left[\begin{array}{c} \bar{I} \\ \bar{J} \\ \bar{K} \end{array} \right] \quad (4)$$

At time t_1+h , they are related by the new direction cosine matrix $[a_{mn}(t_1+h)]$.

$$\left[\begin{array}{c} \bar{i}(t_1+h) \\ \bar{j}(t_1+h) \\ \bar{k}(t_1+h) \end{array} \right] = \left[\begin{array}{ccc} a_{11}(t_1+h) & a_{12}(t_1+h) & a_{13}(t_1+h) \\ a_{21}(t_1+h) & a_{22}(t_1+h) & a_{23}(t_1+h) \\ a_{31}(t_1+h) & a_{32}(t_1+h) & a_{33}(t_1+h) \end{array} \right] \left[\begin{array}{c} \bar{I} \\ \bar{J} \\ \bar{K} \end{array} \right] \quad (5)$$

It can be assumed that this small time increment changes are linear, therefore

$$\begin{bmatrix} \bar{i}(t_1+h) \\ \bar{j}(t_1+h) \\ \bar{k}(t_1+h) \end{bmatrix} = \begin{bmatrix} \bar{i}(t_1) \\ \bar{j}(t_1) \\ \bar{k}(t_1) \end{bmatrix} + \begin{bmatrix} \Delta \bar{i}(t_1) \\ \Delta \bar{j}(t_1) \\ \Delta \bar{k}(t_1) \end{bmatrix} \quad (6)$$

From Eqs. (3) - (6), one obtains the recursive formula.

$$\begin{bmatrix} a_{11}(t_1+h) & a_{12}(t_1+h) & a_{13}(t_1+h) \\ a_{21}(t_1+h) & a_{22}(t_1+h) & a_{23}(t_1+h) \\ a_{31}(t_1+h) & a_{32}(t_1+h) & a_{33}(t_1+h) \end{bmatrix} = \left(\begin{bmatrix} 1 & 0 & 0 \\ 0 & 1 & 0 \\ 0 & 0 & 1 \end{bmatrix} + h \begin{bmatrix} 0 & w_3(t_1) & -w_2(t_1) \\ -w_3(t_1) & 0 & w_1(t_1) \\ w_2(t_1) & -w_1(t_1) & 0 \end{bmatrix} \right) \begin{bmatrix} a_{11}(t_1) & a_{12}(t_1) & a_{13}(t_1) \\ a_{21}(t_1) & a_{22}(t_1) & a_{23}(t_1) \\ a_{31}(t_1) & a_{32}(t_1) & a_{33}(t_1) \end{bmatrix} \quad (7)$$

or in simple form,

$$[A(t_1+h)] = ([I] + h[\Omega(t_1)])[A(t_1)] \quad (8)$$

Since matrix A is self-adjoint [8], i.e., the inverse of the matrix is equal to the transpose, matrix B

$$B(t_1+h) = A^T(t_1+h) \quad (9)$$

is used to rotate the moving coordinate components into the fixed coordinate components.

The accuracy of the transformation matrices A and B can be checked by using the orthonormal relationship [8] of the square root sum of the direction cosines of any vector being unity, e.g., $\sqrt{a_{11}^2+a_{12}^2+a_{13}^2}=1$, $\sqrt{a_{12}^2+a_{22}^2+a_{32}^2}=1$, etc.

Equation (7) can also be derived from the yaw-pitch-roll transformation matrix [8]

$$\begin{bmatrix} \cos P \cos Y & \cos P \sin Y & -\sin P \\ -\sin Y \cos R & \cos Y \cos R & \cos P \sin R \\ +\sin R \sin P \cos Y & +\sin R \sin P \sin Y & \\ \sin Y \sin R & -\sin R \cos Y & \cos P \cos R \\ +\cos R \sin P \cos Y & +\cos R \sin P \sin Y & \end{bmatrix}$$

When the angles are small, the transformation matrix becomes

$$\begin{bmatrix} 1 & Y & -P \\ -Y & 1 & R \\ P & -R & 1 \end{bmatrix}$$

which is identical to that of Eq. (7).

Laboratory Coordinate Data

Using this simple rotational coordinate transformation technique, the angular kinematics and the linear kinematics in the Laboratory coordinate are shown in Figs. 17 and 18 respectively.

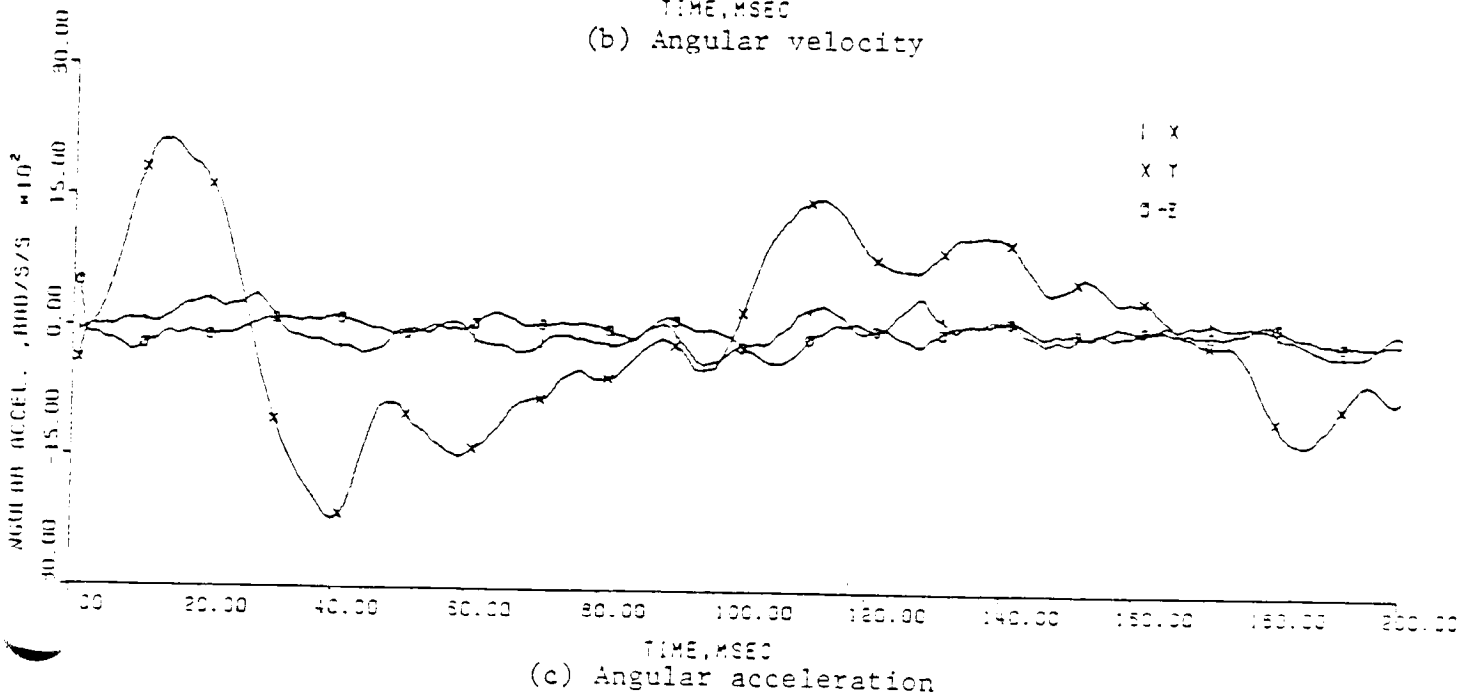
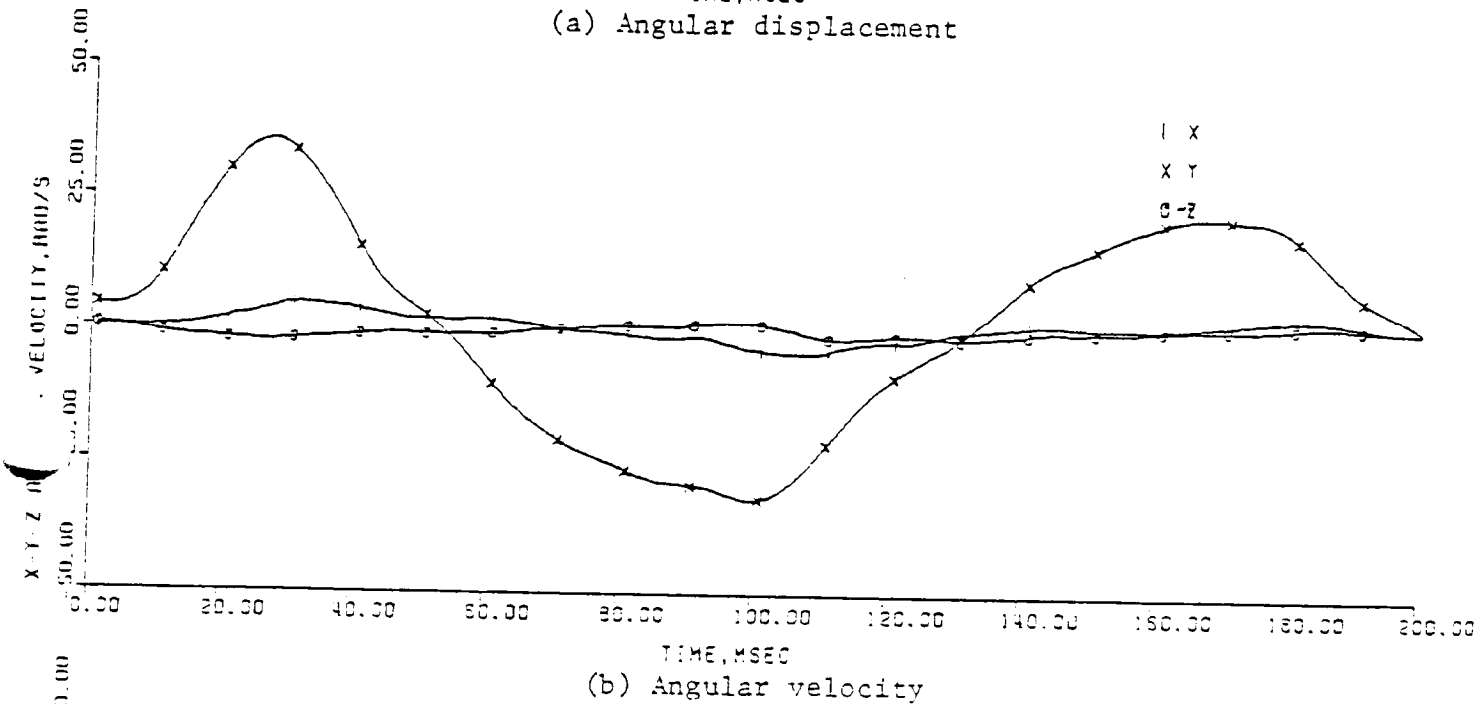
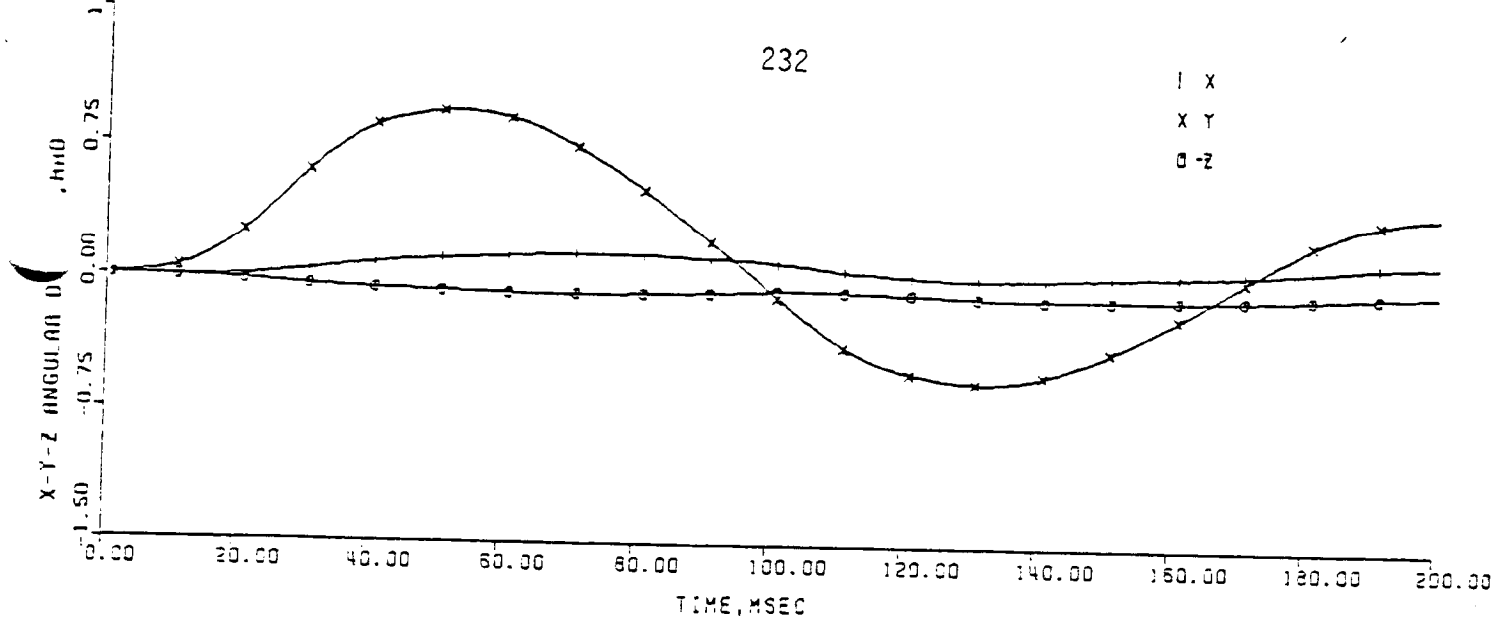


Fig. 17. Transducer angular data in laboratory coordinate.

| X
X Y
O-Z

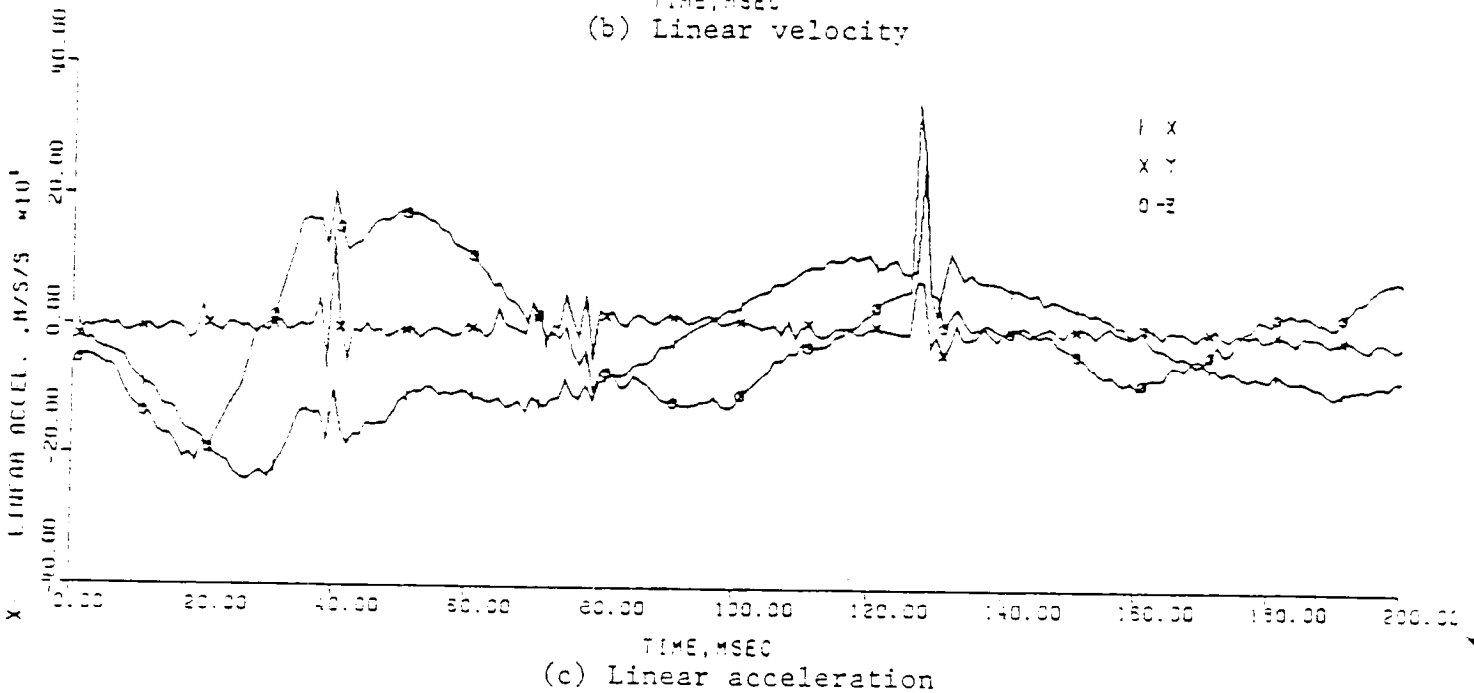
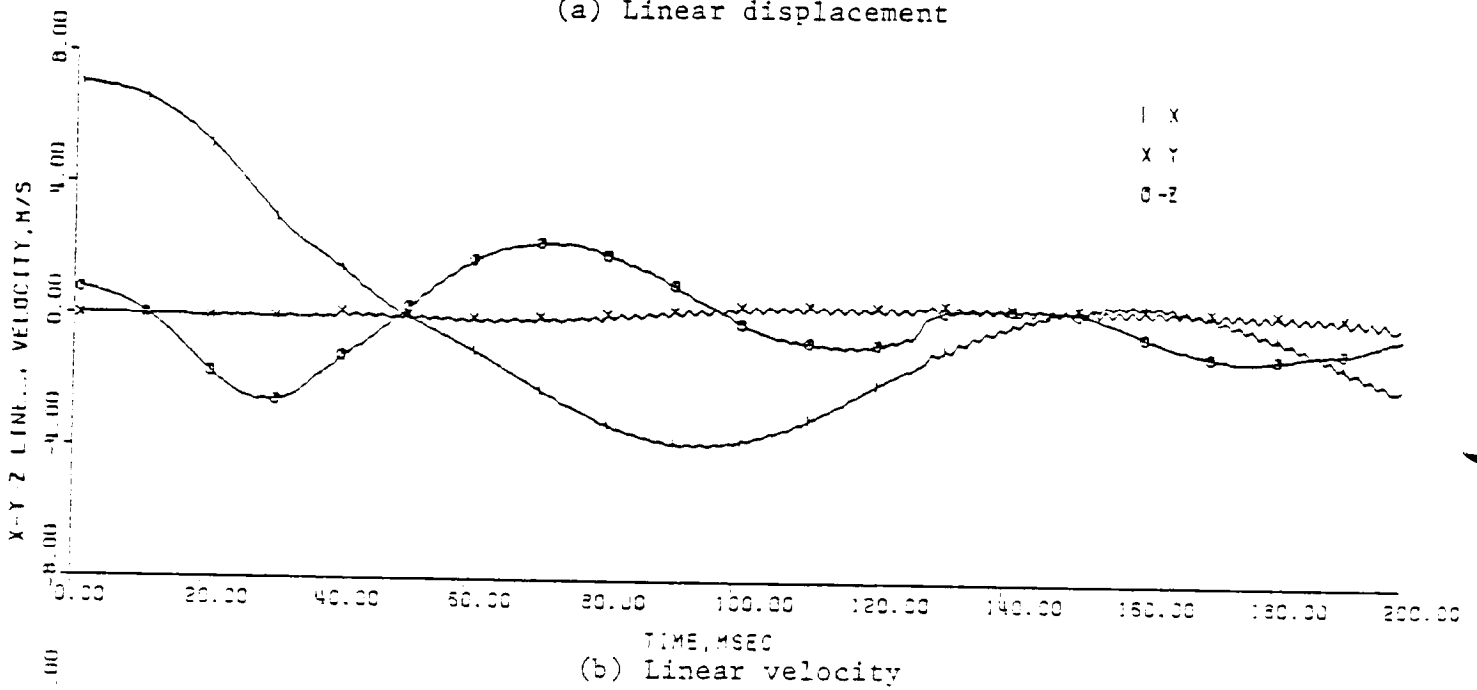
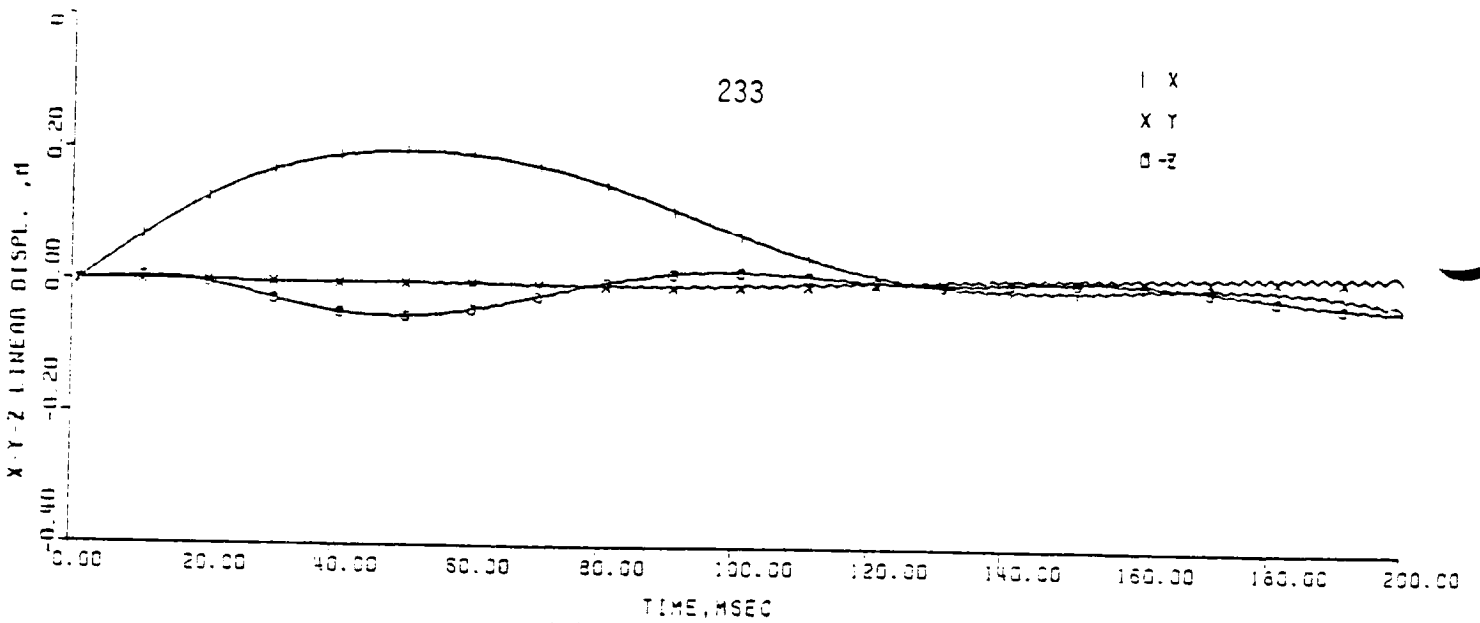


Fig. 18. Transducer linear data in laboratory coordinate.

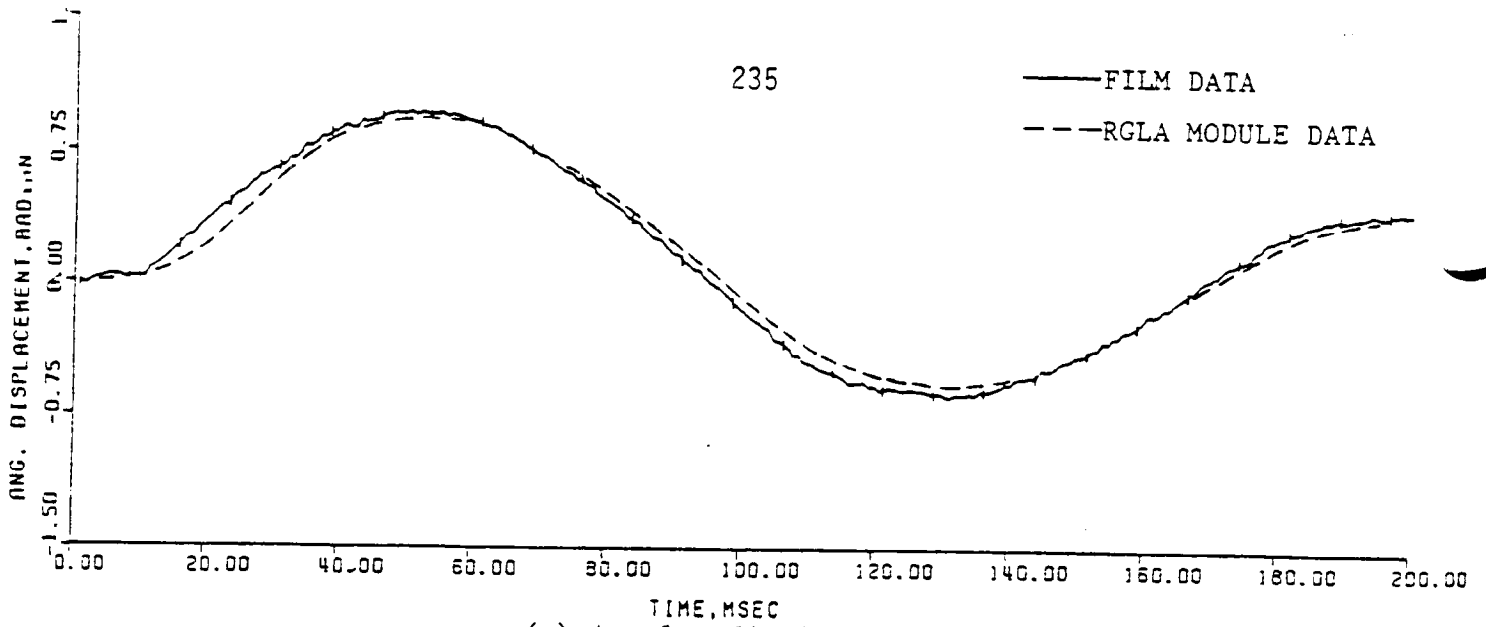
The comparison of the transducer data and the film data is presented in Figs. 19 and 20. Figure 19 shows the good angular correlation between these two measurements. Figure 20 also shows good linear correlation. There are some minor deviations. They could be caused by a combination of angular kinematic error, accelerometer calibration error, accelerometer bias error, alignment error, computation cumulative error, digitization (7-bit) error, initial condition (velocity and position) error, etc.

KINEMATIC EFFECT DUE TO MODULE WEIGHT

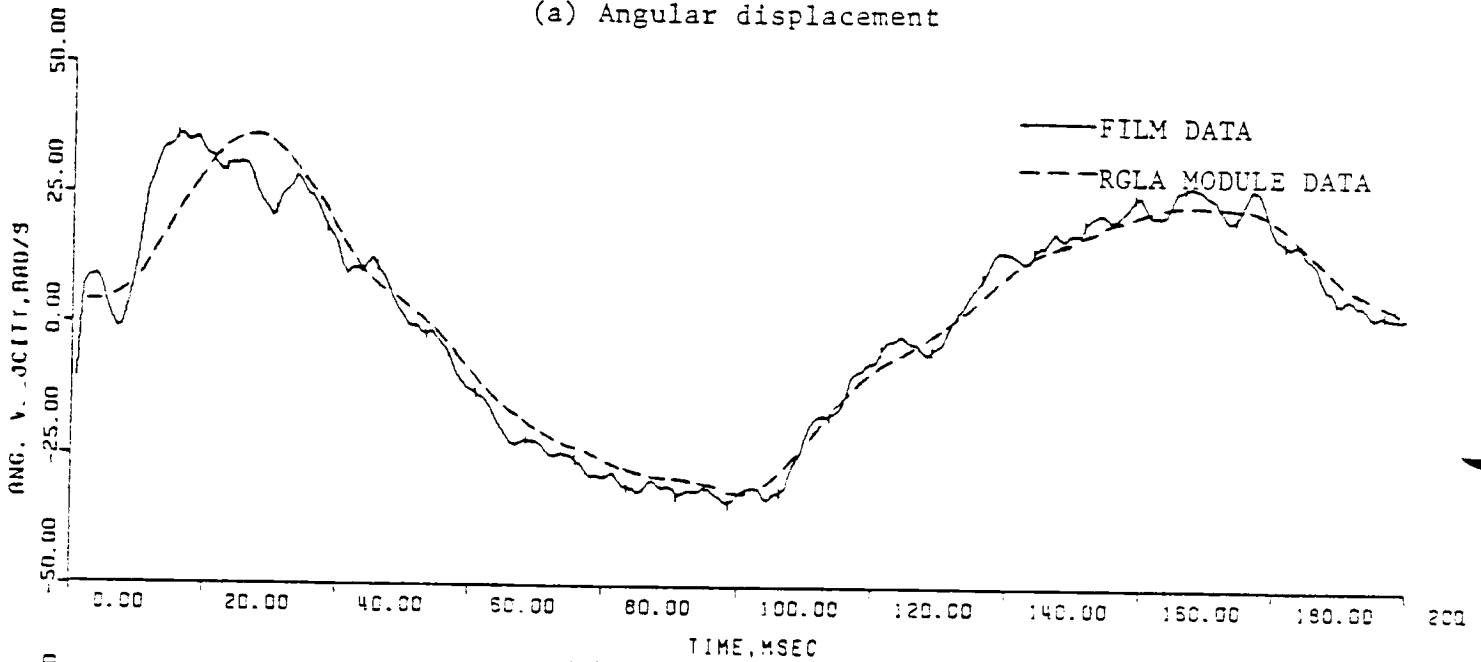
The gyro-accelerometer module used for the 2-D application weighs 6 ounces. It is approximately 5% of an average head weight and, therefore, it has no significant weight effect. In the gyro-accelerometer module for 3-D application (three gyros and three accelerometers), both experimental and computer methods were used to study the kinematic effect due to the module weight. A 3-D module will weigh 12 ounces.

Pendulum Test

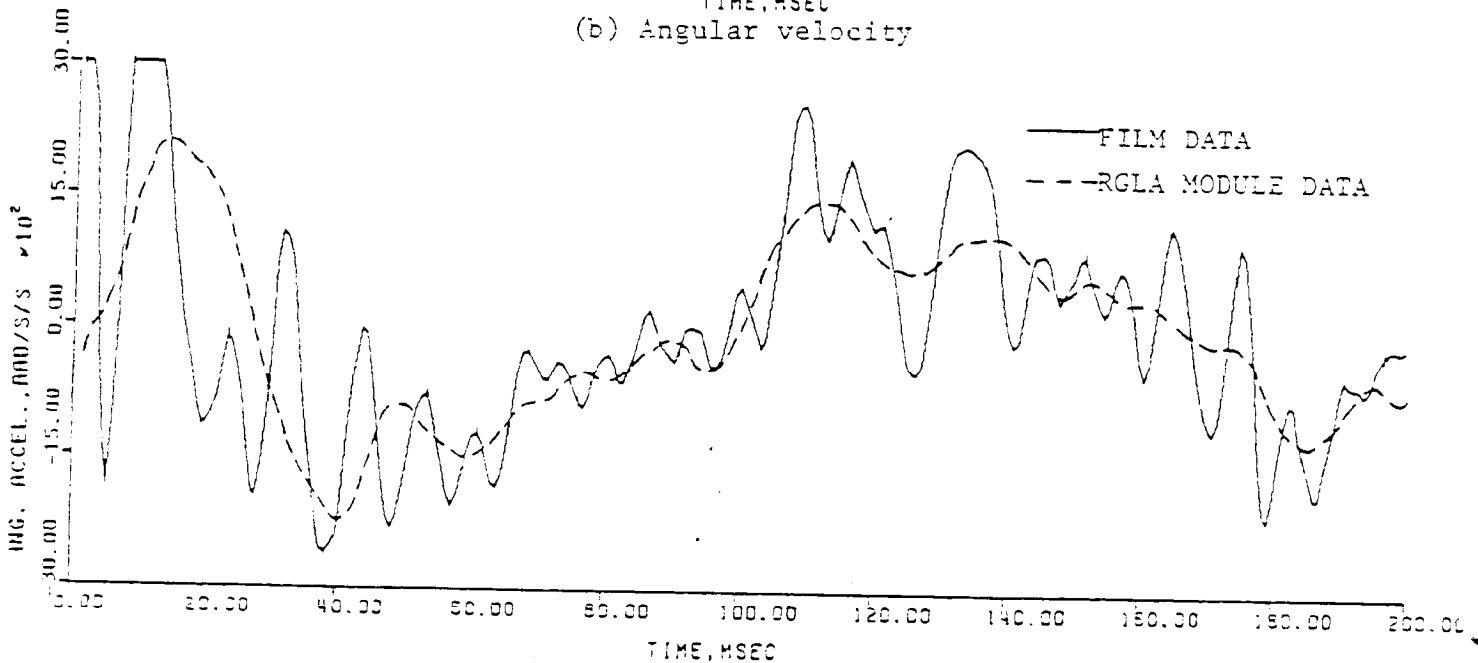
A 572 dummy head-neck assembly [2] was mounted on a component test pendulum with the mid-sagittal plane perpendicular to the plane of motion. The head response due to a 20 fps side impact was photographed by a high-speed camera. The second run, with a one-pound weight attached to the temple of the head C.G., was similarly conducted. The results of these two runs are compared in the following table.



(a) Angular displacement



(b) Angular velocity

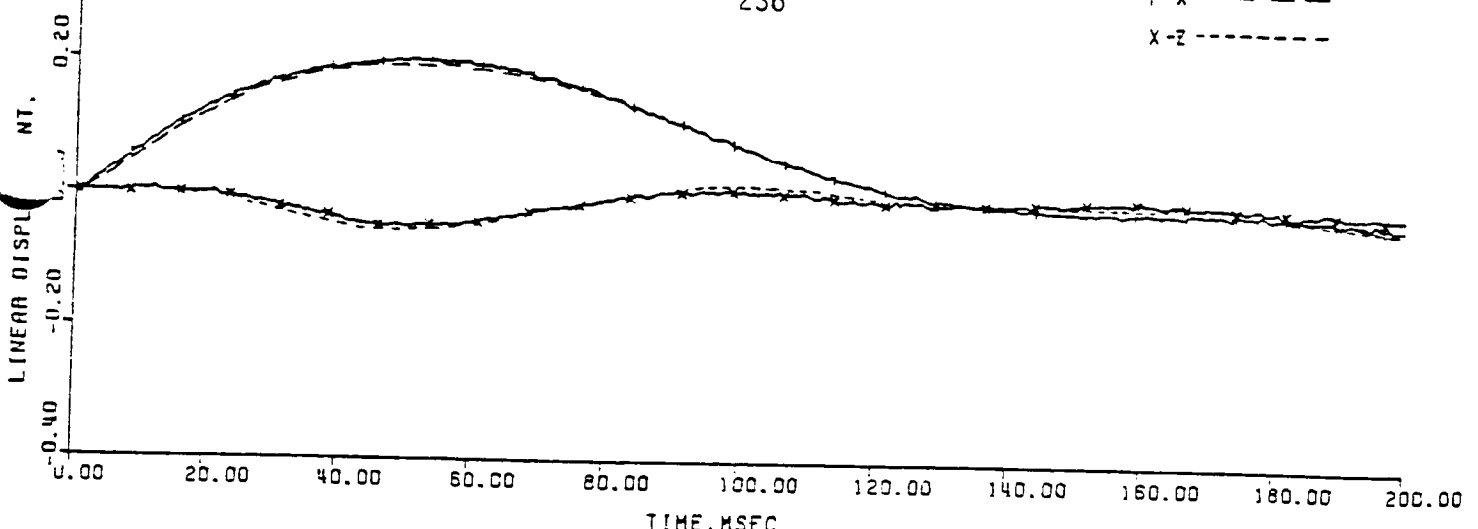


(c) Angular acceleration

Fig. 19. Comparison of angular data in laboratory coordinate.

X - - - -

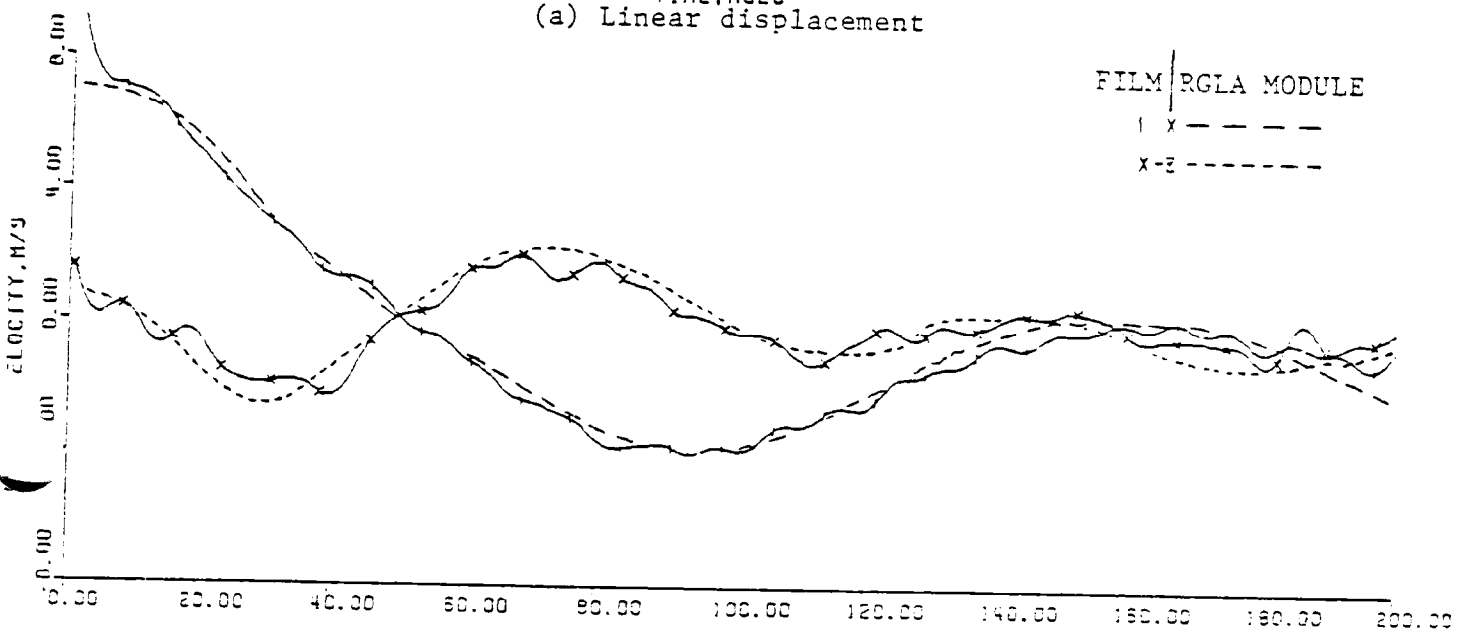
X-Z - - - - -



(a) Linear displacement

X - - - -

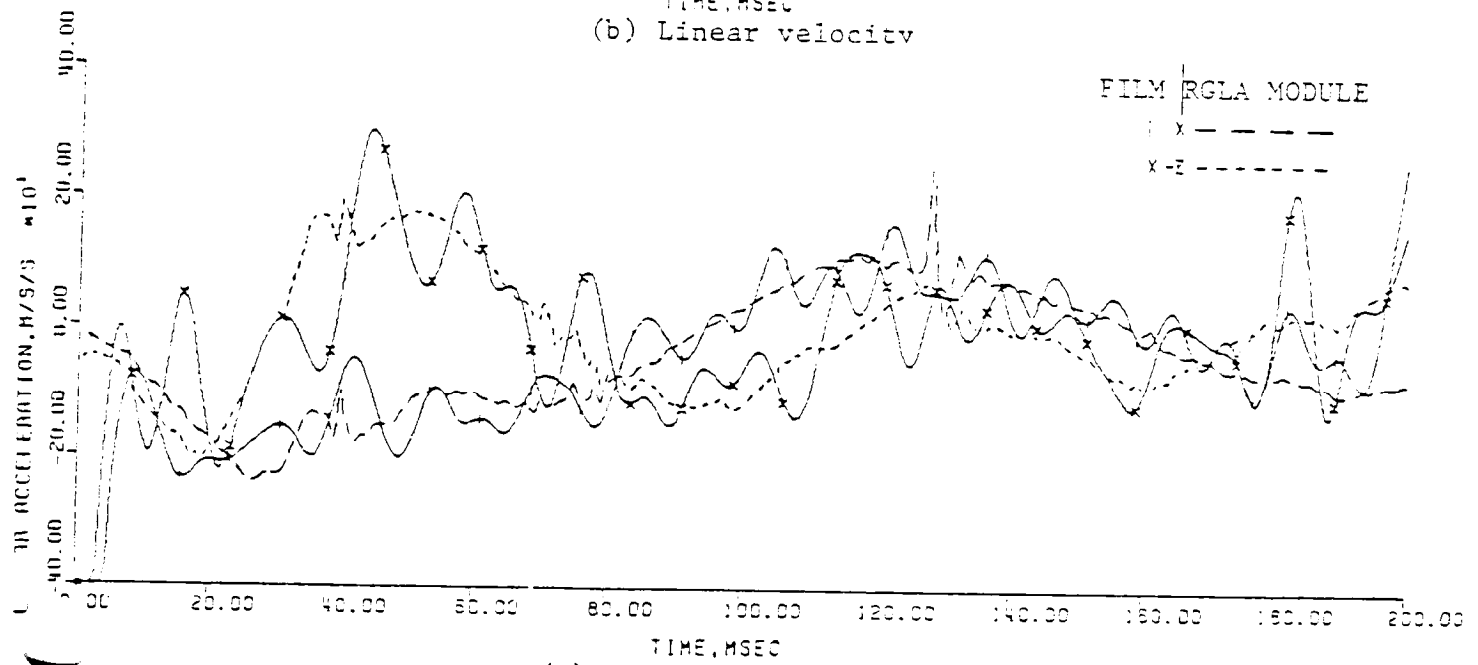
X-Z - - - - -



(b) Linear velocity

X - - - -

X-Z - - - - -



(c) Linear acceleration

Fig. 20. Comparison of linear data in laboratory coordinate.

ITEM	WITHOUT ADDITIONAL WEIGHT	WITH ADDITIONAL 1-LB WEIGHT	% CHANGE
Maximum head rotation	70 deg.	73.2 deg.	4.6
Maximum chordal displacement	6.02 inch	6.38 inch	6.0

This experiment indicates that a one-pound instrumentation weight does not significantly alter the head-neck impact response characteristics. The effect of this additional weight may be considered as a tolerable error.

Note that the weight of the gyro-accelerometer module can be reduced to approximately 0.5 pound by using one two-axis magneto-hydrodynamic angular rate sensor (2.5 oz.), one single-axis superjet angular rate sensor (1.5 oz.), three single-axis linear accelerometers (1 gram each), and the bracket. All these sensors are commercially available.

Computer Simulation

Two Calspan 3-D computer simulation runs were conducted by Mr. William Bowman of AMRL/BB, Wright-Patterson AFB, to study the effects of a 0.75-pound weight attached to the top of the head. This was a 30-mph frontal crash with the test subject (50th-percentile male dummy) wearing a lap-belt. Figure 21 compares the head angular acceleration of the two runs, with and without the additional weight, under same impact conditions. The results indicated that when the weight was attached, the peak magnitude error was 3% and the time delay was one millisecond.

This simulation result suggests that a 0.75-pound instrumentation weight

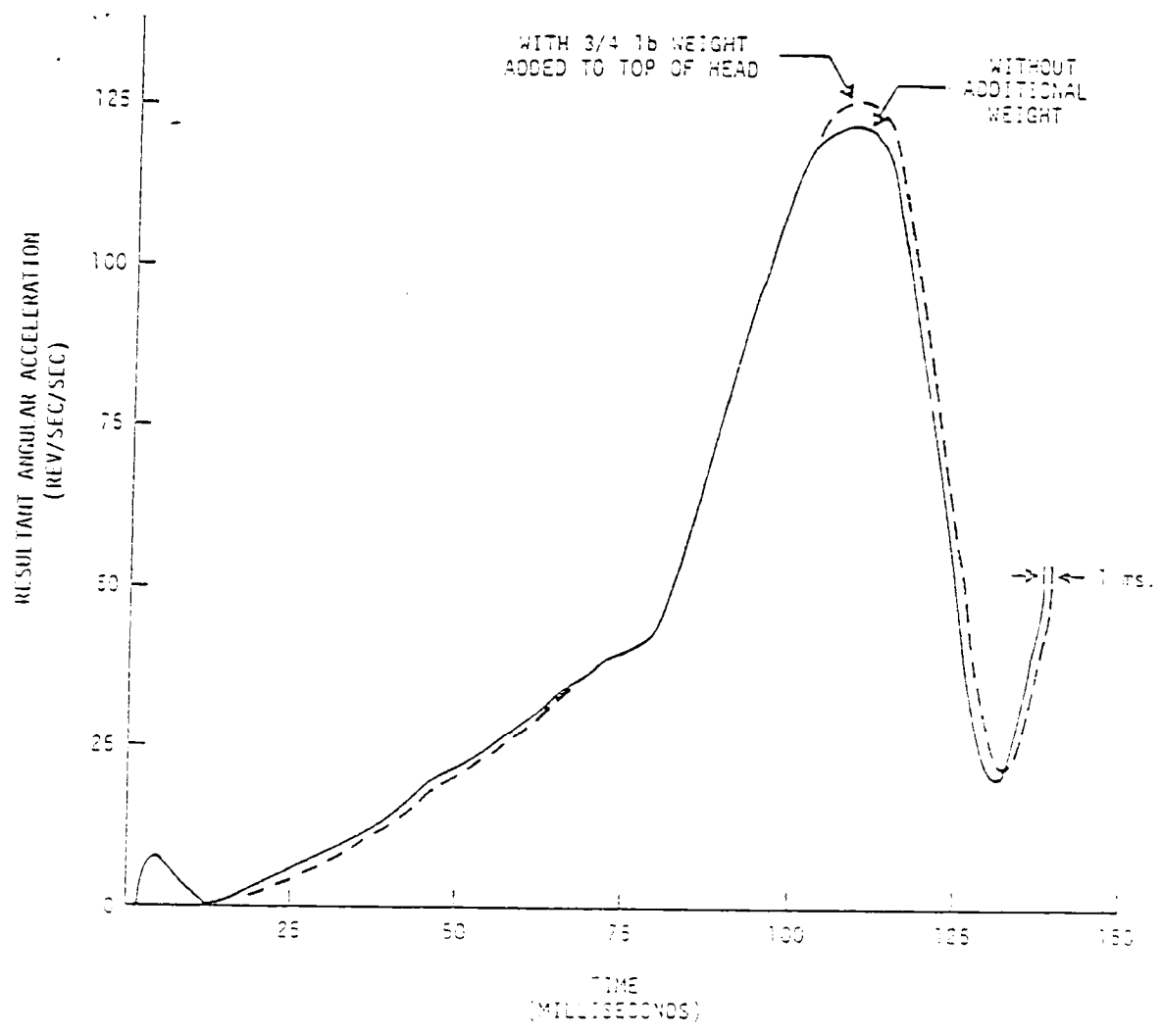


Fig. 21. Effect of RGLA module weight.

attached to the top of the head does not alter the impact response beyond engineering measurement tolerance. Again, the actual module may be attached adjacent to the head C.G., rather than on top of the head. This will further reduce the weight effect.

CONCLUSIONS

An instrumentation module using three rate gyros and three linear accelerometers has been devised and tested. The impact pendulum 2-D model test indicated good correlation of the angular data (displacement, velocity, and acceleration) between the transducer data and the film data. No linear data were studied in this test. Similar 2-D model results had been presented elsewhere [9].

Harmonic analysis indicated that the comparison of the transducer data and the film data were valid because their frequency bandwidths and data rate were sufficiently high to allow differentiations.

The pendulum 3-D model test results, as compared with the film data, also indicated that good six degree-of-freedom kinematic correlations can be obtained. Minor deviations could be caused by a combination of angular kinematic error, accelerometer calibration error, accelerometer bias error, alignment error, initial condition (velocity and displacement) error, etc.

The following technical areas are suggested for future work:

1. Transducers, especially rate gyros, should be examined to determine their sensitivity to linear accelerations. A market survey should also be conducted to find the state-of-the-art angular rate sensors.
2. This RGLA module performance should be examined in a true 3-D impact environment.
3. This RGLA module should be mounted outside of the head CG of an anthropomorphic dummy, and compare the calculated data at the head CG with those measured at the head CG by other transducers.
4. Methods of rotating coordinate transformation should be studied or devised in order to provide the best accuracy.
5. Error analysis using mathematical model and statistic approach should be studied.
6. The digitization accuracy should be better than the current 1% accuracy (limited by the 7-bit word PCM data system).

REFERENCES

- [1] A. J. Padgoankar, K. W. Krieger, and A. I. King, "measurement of Angular Acceleration of a Rigid Body Using Linear Accelerometers", J. of Applied Mechanics, pp. 552-556, September 1975.

- [2] "Anthropomorphic Test Dummy", Chapter V, Part 572, Federal Register, Vol. 38, No. 147, August 1, 1973. Amended 49CFR Part 572, Federal Register, Vol. 40, No. 154, August 8, 1975.
- [3] F. B. Hilderbrand, Introduction to Numerical Analysis, McGraw-Hill, New York, 1956.
- [4] C. Lanczos, Applied Analysis, Prentice Hall, New Jersey, 1956.
- [5] R. C. Haut, E. P. Remmers, and W. W. Meyer, "A Numerical Method of Film Analysis with Differentiation with Application in Biomechanics", Proc. Soc. Photo-optical Instrumentation Engineers, Vol. 57, pp. 53-61, 1974.
- [6] A. S. Hu and H. T. Chen, "Frequency Response and Differentiation Requirements for Impact Measurements", submitted to Shock and Vibration Bulletin, 1977.
- [7] M. R. Spiegel, Theoretical Mechanics, Ch. 5 McGraw-hill, New York, 1967.
- [8] G. R. Macomber and M. Fernandez, Inertial Guidance Engineering, Ch. 2, Prentice-Hall, Englewood Cliffs, N. J., 1962.
- [9] A. S. Hu, S. P. Bean, and R. M. Zimmerman, "Response of Belted Dummy and Cadaver to Rear Impact", Technical Report, Physical Science Laboratory, New Mexico State University, July 1976.